Pulse–chase analysis

HEK293T cells stably expressing Flag-UCH37 were transfected with siRNA for hRpn13 or control siRNA. Pulse–chase experiments were performed as described previously (Hirano *et al*, 2005).

RT–PCR analysis

Total RNA (2.5 μg) was reverse transcribed using SuperScript III (Invitrogen) and oligo$(dT)_{20}$ primers. Specific primers for each gene were as follows: 5′-AAGGATCCATGAGCATCCTGGCCACG ATGAACG-3′ and 5′-TTCTCGAGTCAGTCCAGGCTCATGTCCTCC-3′ for hRpn13, 5′-AAGGATCCATGACGGGCAACGCCGGGGAG-3′ and 5′-TTCTCGAGTCATTTGGTTTCCTGAGCTTTC-3′ for UCH37, and 5′-ACCACAGTCCATGCCATCAC-3′ and 5′-TCCACCACCCTGTTGCT GTA-3′ for G3PDH.

Supplementary data

Supplementary data are available at *The EMBO Journal* Online (http://www.embojournal.org).

Acknowledgements

We thank Y Murakami for providing the ODC degradation assay system and K Furuyama for technical support. This work was supported in part by a grant to SM from JST and grants to SM and KT from the Ministry of Education, Science and Culture of Japan.

References

Anderson C, Crimmins S, Wilson JA, Korbel GA, Ploegh HL, Wilson SM (2005) Loss of Usp14 results in reduced levels of ubiquitin in ataxia mice. *J Neurochem* **95:** 724–731

Baumeister W, Walz J, Zuhl F, Seemuller E (1998) The proteasome: paradigm of a self-compartmentalizing protease. *Cell* **92:** 367–380

Coux O, Tanaka K, Goldberg AL (1996) Structure and functions of the 20S and 26S proteasomes. *Annu Rev Biochem* **65:** 801–847

Glickman MH, Ciechanover A (2002) The ubiquitin-proteasome proteolytic pathway: destruction for the sake of construction. *Physiol Rev* **82:** 373–428

Glickman MH, Rubin DM, Coux O, Wefes I, Pfeifer G, Cjeka Z, Baumeister W, Fried VA, Finley D (1998) A subcomplex of the proteasome regulatory particle required for ubiquitin-conjugate degradation and related to the COP9-signalosome and eIF3. *Cell* **94:** 615–623

Guerrero C, Tagwerker C, Kaiser P, Huang L (2006) An integrated mass spectrometry-based proteomic approach. *Mol Cell Proteomics* **5:** 366–378

Guterman A, Glickman MH (2004) Complementary roles for Rpn11 and Ubp6 in deubiquitination and proteolysis by the proteasome. *J Biol Chem* **279:** 1729–1738

Hasegawa K, Sakurai N, Kinoshita T (2001) Xoom is maternally stored and functions as a transmembrane protein for gastrulation movement in *Xenopus* embryos. *Dev Growth Differ* **43:** 25–31

Hirano Y, Hendil KB, Yashiroda H, Iemura S, Nagane R, Hioki Y, Natsume T, Tanaka K, Murata S (2005) A heterodimeric complex that promotes the assembly of mammalian 20S proteasomes. *Nature* **437:** 1381–1385

Holzl H, Kapelari B, Kellermann J, Seemuller E, Sumegi M, Udvardy A, Medalia O, Sperling J, Muller SA, Engel A, Baumeister W (2000) The regulatory complex of *Drosophila melanogaster* 26S proteasomes. Subunit composition and localization of a deubiquitylating enzyme. *J Cell Biol* **150:** 119–130

Ito T, Chiba T, Ozawa R, Yoshida M, Hattori M, Sakaki Y (2001) A comprehensive two-hybrid analysis to explore the yeast protein interactome. *Proc Natl Acad Sci USA* **98:** 4569–4574

Jorgensen JP, Lauridsen AM, Kristensen P, Dissing K, Johnsen AH, Hendil KB, Hartmann-Petersen R (2006) Adrm1, a putative adhesion regulating protein, is a novel proteasome-associated factor. *J Mol Biol* **360:** 1043–1052

Komatsu M, Waguri S, Ueno T, Iwata J, Murata S, Tanida I, Ezaki J, Mizushima N, Ohsumi Y, Uchiyama Y, Kominami E, Tanaka K, Chiba T (2005) Impairment of starvation-induced and constitutive autophagy in Atg7-deficient mice. *J Cell Biol* **169:** 425–434

Kumatori A, Tanaka K, Inamura N, Sone S, Ogura T, Matsumoto T, Tachikawa T, Shin S, Ichihara A (1990) Abnormally high expression of proteasomes in human leukemic cells. *Proc Natl Acad Sci USA* **87:** 7071–7075

Lam YA, Xu W, DeMartino GN, Cohen RE (1997) Editing of ubiquitin conjugates by an isopeptidase in the 26S proteasome. *Nature* **385:** 737–740

Lamerant N, Kieda C (2005) Adhesion properties of adhesion-regulating molecule 1 protein on endothelial cells. *FEBS J* **272:** 1833–1844

Leggett DS, Hanna J, Borodovsky A, Crosas B, Schmidt M, Baker RT, Walz T, Ploegh H, Finley D (2002) Multiple associated proteins regulate proteasome structure and function. *Mol Cell* **10:** 495–507

Li T, Duan W, Yang H, Lee MK, Bte Mustafa F, Lee BH, Teo TS (2001) Identification of two proteins, S14 and UIP1, that interact with UCH37. *FEBS Lett* **488:** 201–205

Li T, Naqvi NI, Yang H, Teo TS (2000) Identification of a 26S proteasome-associated UCH in fission yeast. *Biochem Biophys Res Commun* **272:** 270–275

MacArthur MW, Thornton JM (1991) Influence of proline residues on protein conformation. *J Mol Biol* **218:** 397–412

Murakami Y, Matsufuji S, Kameji T, Hayashi S, Igarashi K, Tamura T, Tanaka K, Ichihara A (1992) Ornithine decarboxylase is degraded by the 26S proteasome without ubiquitination. *Nature* **360:** 597–599

Murata S, Minami Y, Minami M, Chiba T, Tanaka K (2001) CHIP is a chaperone-dependent E3 ligase that ubiquitylates unfolded protein. *EMBO Rep* **2:** 1133–1138

Natsume T, Yamauchi Y, Nakayama H, Shinkawa T, Yanagida M, Takahashi N, Isobe T (2002) A direct nanoflow liquid chromatography-tandem mass spectrometry system for interaction proteomics. *Anal Chem* **74:** 4725–4733

Realini C, Rogers SW, Rechsteiner M (1994) KEKE motifs. Proposed roles in protein–protein association and presentation of peptides by MHC class I receptors. *FEBS Lett* **348:** 109–113

Shimada S, Ogawa M, Schlom J, Greiner JW (1991) Identification of a novel tumor-associated Mr 110 000 gene product in human gastric carcinoma cells that is immunologically related to carcinoembryonic antigen. *Cancer Res* **51:** 5694–5703

Shimada S, Ogawa M, Takahashi M, Schlom J, Greiner JW (1994) Molecular cloning and characterization of the complementary DNA of an M(r) 110 000 antigen expressed by human gastric carcinoma cells and upregulated by gamma-interferon. *Cancer Res* **54:** 3831–3836

Simins AB, Weighardt H, Weidner KM, Weidle UH, Holzmann B (1999) Functional cloning of ARM-1, an adhesion-regulating molecule upregulated in metastatic tumor cells. *Clin Exp Metast* **17:** 641–648

Smith DM, Kafri G, Cheng Y, Ng D, Walz T, Goldberg AL (2005) ATP binding to PAN or the 26S ATPases causes association with the 20S proteasome, gate opening, and translocation of unfolded proteins. *Mol Cell* **20:** 687–698

Stone M, Hartmann-Petersen R, Seeger M, Bech-Otschir D, Wallace M, Gordon C (2004) Uch2/Uch37 is the major deubiquitinating enzyme associated with the 26S proteasome in fission yeast. *J Mol Biol* **344:** 697–706

Suzuki H, Chiba T, Suzuki T, Fujita T, Ikenoue T, Omata M, Furuichi K, Shikama H, Tanaka K (2000) Homodimer of two F-box proteins βTrCP1 or βTrCP2 binds to IκBα for signal-dependent ubiquitination. *J Biol Chem* **275:** 2877–2884

Verma R, Aravind L, Oania R, McDonald WH, Yates III JR, Koonin EV, Deshaies RJ (2002) Role of Rpn11 metalloprotease in deubiquitination and degradation by the 26S proteasome. *Science* **298:** 611–615

Verma R, Chen S, Feldman R, Schieltz D, Yates J, Dohmen J, Deshaies RJ (2000) Proteasomal proteomics: identification of nucleotide-sensitive proteasome-interacting proteins by mass spectrometric analysis of affinity-purified proteasomes. *Mol Biol Cell* **11:** 3425–3439

Verma R, Oania R, Graumann J, Deshaies RJ (2004) Multiubiquitin chain receptors define a layer of substrate selectivity in the ubiquitin-proteasome system. *Cell* **118:** 99–110

Winzeler EA, Shoemaker DD, Astromoff A, Liang H, Anderson K, Andre B, Bangham R, Benito R, Boeke JD, Bussey H, Chu AM, Connelly C, Davis K, Dietrich F, Dow SW, El Bakkoury M, Foury F, Friend SH, Gentalen E, Giaever G, Hegemann JH, Jones T, Laub M, Liao H, Liebundguth N, Lockhart DJ, Lucau-Danila A, Lussier M, M'Rabet N, Menard P, Mittmann M, Pai C, Rebischung C, Revuelta JL, Riles L, Roberts CJ, Ross-MacDonald P, Scherens B, Snyder M, Sookhai-Mahadeo S, Storms RK, Veronneau S, Voet M, Volckaert G, Ward TR, Wysocki R, Yen GS, Yu K, Zimmermann K, Philippsen P, Johnston M, Davis RW (1999) Functional characterization of the *S. cerevisiae* genome by gene deletion and parallel analysis. *Science* **285:** 901–906

Yang Y, Fang S, Jensen JP, Weissman AM, Ashwell JD (2000) Ubiquitin protein ligase activity of IAPs and their degradation in proteasomes in response to apoptotic stimuli. *Science* **288:** 874–877

Yao T, Cohen RE (2002) A cryptic protease couples deubiquitination and degradation by the proteasome. *Nature* **419:** 403–407

nature
cell biology

SUMO-specific protease SUSP4 positively regulates p53 by promoting Mdm2 self-ubiquitination

Moon Hee Lee[1], Sung Won Lee[1], Eun Joo Lee[1], Soo Joon Choi[1], Sung Soo Chung[1], Jae Il Lee[2], Joong Myung Cho[2], Jae Hong Seol[1], Sung Hee Baek[1], Keun Il Kim[3], Tomoki Chiba[4], Keiji Tanaka[4], Ok Sun Bang[1,5] and Chin Ha Chung[1,5]

The p53 tumour suppressor has a key role in the control of cell growth and differentiation, and in the maintenance of genome integrity[1,2]. p53 is kept labile under normal conditions, but in response to stresses, such as DNA damage, it accumulates in the nucleus for induction of cell-cycle arrest, DNA repair or apoptosis. Mdm2 is an ubiquitin ligase that promotes p53 ubiquitination and degradation[3–5]. Mdm2 is also self-ubiquitinated and degraded. Here, we identified a novel cascade for the increase in p53 level in response to DNA damage. A new SUMO-specific protease, SUSP4, removed SUMO-1 from Mdm2 and this desumoylation led to promotion of Mdm2 self-ubiquitination, resulting in p53 stabilization. Moreover, SUSP4 competed with p53 for binding to Mdm2, also resulting in p53 stabilization. Overexpression of SUSP4 inhibited cell growth, whereas knockdown of *susp4* by RNA interference (RNAi) promoted of cell growth. UV damage induced SUSP4 expression, leading to an increase in p53 levels in parallel with a decrease in Mdm2 levels. These findings establish a new mechanism for the elevation of cellular p53 levels in response to UV damage.

Small ubiquitin-related modifier (SUMO) is an ubiquitin-like protein that is conjugated to a variety of cellular proteins[6,7]. Similarly to ubiquitination, sumoylation occurs through three enzymatic steps catalysed by the E1 enzyme Sae1–Sae2, the E2 enzyme Ubc9, and the E3 ligases, including RanBP2 (ref. 8), Pc2 (ref. 9) and PIASs[10,11]. Protein sumoylation participates in the control of diverse cellular processes, including transcriptional regulation, nuclear transport and signal transduction[12–14]. SUMO modification is a reversible process that is catalysed by a family of SUMO-specific proteases. In yeast, two SUMO proteases, Ulp1 and Ulp2, have been identified[15,16]. In humans, several SUMO proteases have been identified, including SENP1, 2, 3, 5 and 6 (refs 12, 17, 18).

p53 is modified by SUMO-1 and overexpression of SUMO-1 or Ubc9 was reported to induce an increase in p53-dependent transcription[19,20]. However, it was also reported that sumoylation of p53 has no effects on its transcriptional activity and coexpression of PIAS1 and SUMO-1 instead represses p53 activity[21–23]. Mdm2 is also modified by SUMO-1 (refs 24, 25). Interestingly, the nucleoli tumour suppressor $p19^{ARF}$ (alternative reading frame), which inhibits Mdm2 and thereby stabilizes p53, promotes sumoylation of Mdm2 (refs 24, 25). However, $p19^{ARF}$ recruits Mdm2, Ubc9 and SUMO-1 to the nucleoli[24]. Moreover, the CELO (chicken embryo lethal orphan) adenovirus protein, Gam1 (gallus ante morte 1), which inhibits Sae1–Sae2 (ref. 26) and leads to downregulation of Ubc9, has no overt effect on the ability of $p19^{ARF}$ to activate p53 (ref. 27). Thus, the functional relevance of sumoylation of Mdm2, in addition to p53, in the p53–Mdm2 pathway remained unclear.

EST database searches for mouse genes identified a partial clone that has a homologous sequence encoding the carboxy-terminal catalytic domains of yeast Ulp1 (ref. 15). Based on the sequence of the clone, we isolated a cDNA for SUMO-1-specific protease from mouse brain mRNAs. The cDNA clone contained a 1,500 base-pair open reading frame encoding a protein of 499 amino acids with a predicted relative molecular mass of 54,890 (M_r 54.89K), which we named SUSP4. Similarly to other SUMO proteases, SUSP4 has a conserved His–Asp–Cys catalytic triad (see Supplementary Information, Fig. S1). The C-terminal active-site domain and the remaining amino-terminal region of SUSP4 show approximately 65% and 30% identity with those of human SENP2 and mouse SuPr1, respectively[17,28], suggesting that SUSP4, like SuPr1, is a mouse homologue of SENP2. SUSP4 was ubiquitously expressed in all tissues and cell lines tested, although the protein levels of SUSP4 varied in different tissues and cell lines (see Supplementary Information, Fig. S2).

p53 and Mdm2 were found to interact with SUSP4 on MALDI-TOF mass spectrometric analysis of the proteins that bound to Myc-$SUSP4^{C460S}$ (in which the active site Cys 460 was replaced by Ser), but not to the Myc-tag itself (Fig. 1a). To confirm their interaction, His-tagged SUSP4 and a His tag expressed in *Escherichia coli* (Fig. 1b) were incubated with GST–p53 or MBP–Mdm2. Pulldown assay with NTA resins showed that GST–p53 and MBP–Mdm2 were coprecipitated with His–SUSP4, but not with the His-tag (Fig. 1c), indicating that the proteins directly interact with SUSP4. Immunoprecipitation analysis also revealed that

[1]NRL of Protein Biochemistry, School of Biological Sciences, Seoul National University, Seoul 151-742, Korea. [2]Crystalgenomics Inc., Seoul 138-736, Korea. [3]Department of Biological Sciences, Sookmyung Woman's University, Seoul 140-742, Korea. [4]Tokyo Metropolitan Institute of Medical Sciences, Tokyo 113, Japan. [5]Correspondence should be addressed to C.H.C. or O.S.B. (e-mails: chchung@snu.ac.kr; osbang@snu.ac.kr)

Received 12 July 2006; accepted 9 October 2006; published online 5 November 2006; DOI: 10.1038/ncb1512

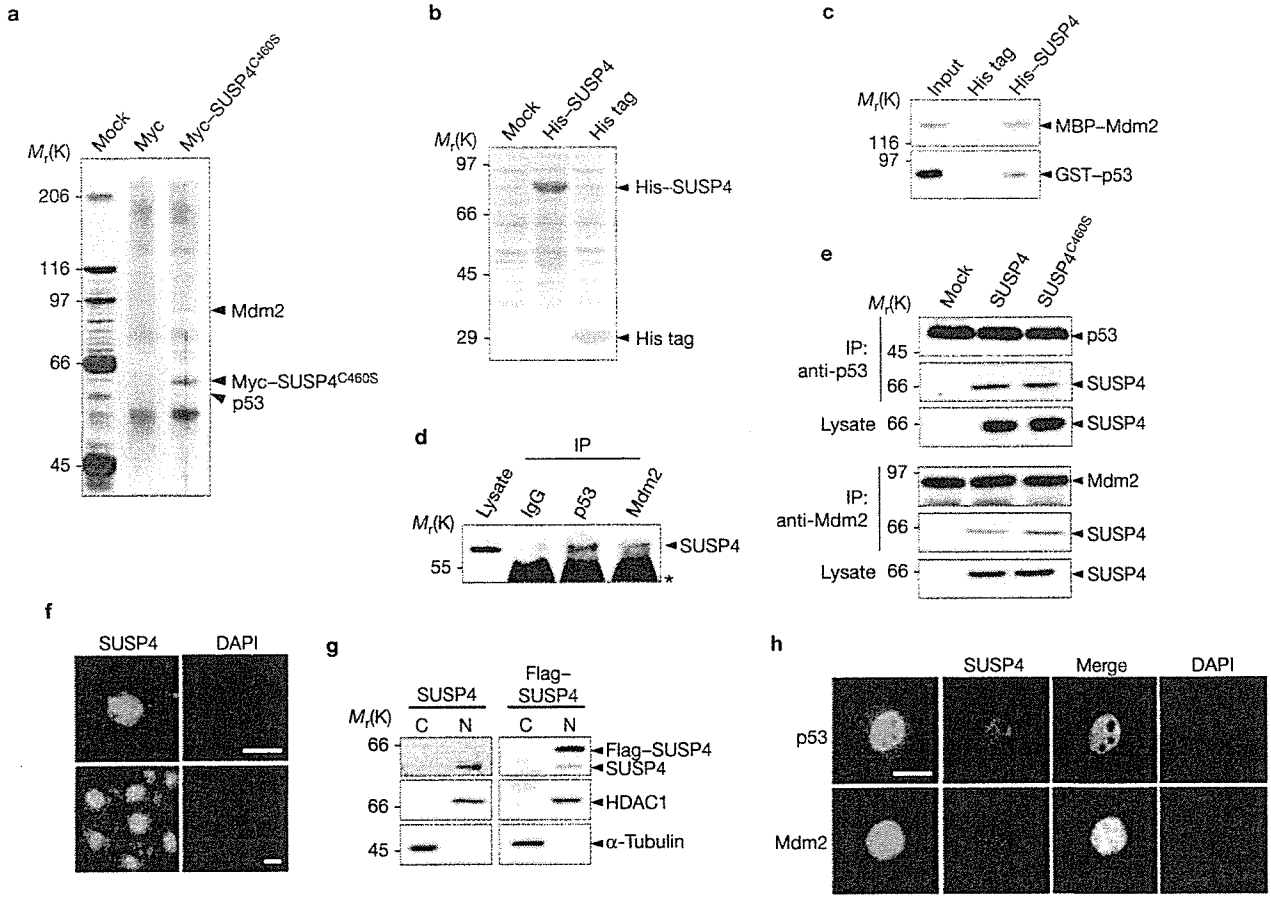

Figure 1 Interaction of SUSP4 with p53 and Mdm2 and their colocalization. (**a**) NIH3T3 cells were transfected with pCMV–Myc or pCMV–Myc–SUSP4^{C460S}. Cell lysates were incubated with Sepharose beads crosslinked with anti-Myc IgG. After washing, bound proteins were released from the beads by boiling, resolved by SDS–PAGE and silver-stained. Protein bands that appeared only in cells expressing Myc–SUSP4^{C460S} were subjected to MALDI-TOF MS analysis. (**b**) His–SUSP4 or His-tag itself were expressed in *E. coli*. Cell extracts were subjected to SDS–PAGE followed by staining with Coomassie blue R-250. (**c**) Purified GST–p53 and MBP–Mdm2 were incubated with the *E. coli* extracts obtained in **b**. After incubation, the samples were treated with NTA resins for 1 h at 4 °C. Precipitates were subjected to SDS–PAGE followed by immunoblot with anti-MBP or anti-GST antibody. Input (20%) indicates the loading controls. (**d**) NIH3T3 cell lysates were subjected to immunoprecipitation with control IgG or anti-p53 or anti-Mdm2 antibody followed by immunoblot with anti-SUSP4 antibody. The asterisk indicates the IgG heavy chain. (**e**) pcDNA–p53 or pcDNA–Mdm2 were transfected into HEK293T cells with pCMV2–Flag–SUSP4, pCMV2–Flag–SUSP4^{C460S} or an empty vector (Mock). After incubation for 24 h, cell lysates were subjected to immunoprecipitation with anti-p53 or anti-Mdm2 antibody followed by immunoblot with anti-Flag antibody. Cells lysates were also directly probed with anti-Flag antibody. (**f**) NIH3T3 cells were stained with purified anti-SUSP4 IgGs. The nuclei were stained with DAPI. The scale bar represents 10 μm. (**g**) Cytosolic (C) and nuclear extracts (N) were prepared from NIH3T3 cells and from the cells that had been transfected with pCMV2–Flag–SUSP4. They were then subjected to immunoblot with anti-SUSP4, anti-HDAC1 or anti-α-tubulin antibodies. (**h**) pCMV–Myc–SUSP4 was transfected to NIH3T3 cells with pcDNA–p53 or pcDNA–Mdm2. After incubation for 24 h, cells were immunostained for Myc–SUSP4 (red) and p53 or Mdm2 (green). They were then observed using a fluorescent microscope. The scale bar represents 10 μm.

endogenous SUSP4 interacts with p53 and Mdm2 (Fig. 1d). Flag-tagged SUSP4 and SUSP4^{C460S} also interacted with ectopically expressed p53 or Mdm2. (Fig. 1e). Immunostaining of cells with purified anti-SUSP4 IgGs showed that endogenous SUSP4 localizes predominantly to the nucleus, although a minor fraction was also observed in the cytoplasm (Fig. 1f). To confirm the localization of SUSP4, cytosolic and nuclear extracts were obtained from NIH3T3 cells and immunoblot analysis of these extracts revealed that both endogenous and ectopically expressed SUSP4 localized predominantly to the nuclear fractions (Fig. 1g). As expected, the marker proteins HDAC1 and α-tubulin were detected in the nuclear and cytosolic fractions, respectively. On overexpression of Myc–SUSP4 with p53 or Mdm2, SUSP4 was found to colocalize with p53 and Mdm2 in the nucleus (Fig. 1h). Collectively, these results demonstrate that SUSP4 interacts with p53 and Mdm2 in the nucleus.

To determine the binding regions of p53 and Mdm2 within SUSP4, His-tagged deletions of SUSP4 were expressed in HEK293T cells with p53 or Mdm2. An SUSP4 truncated mutant containing the N-terminal 200 amino acids (Sd1) interacted with p53, whereas the mutants containing the 201–300 sequence (Sd3 and Sd4) bound to Mdm2 (see Supplementary Information, Fig. S3a). These results indicate that p53 and Mdm2 bind to the N-terminal and middle regions of SUSP4, respectively. To locate the binding regions of SUSP4 within p53 and Mdm2, various deletions of the latter proteins were expressed. The Mdm2 mutants containing the N-terminal 1–158 sequence (Md1 and Md2) interacted with SUSP4 (see Supplementary Information, Fig. S3b), and the p53 mutants carrying the C-terminal 301–393 sequence (Pd3 and Pd4) bound to SUSP4 (see Supplementary Information, Fig. S3c). These results indicate that the SUSP4-binding sites reside within the N- and

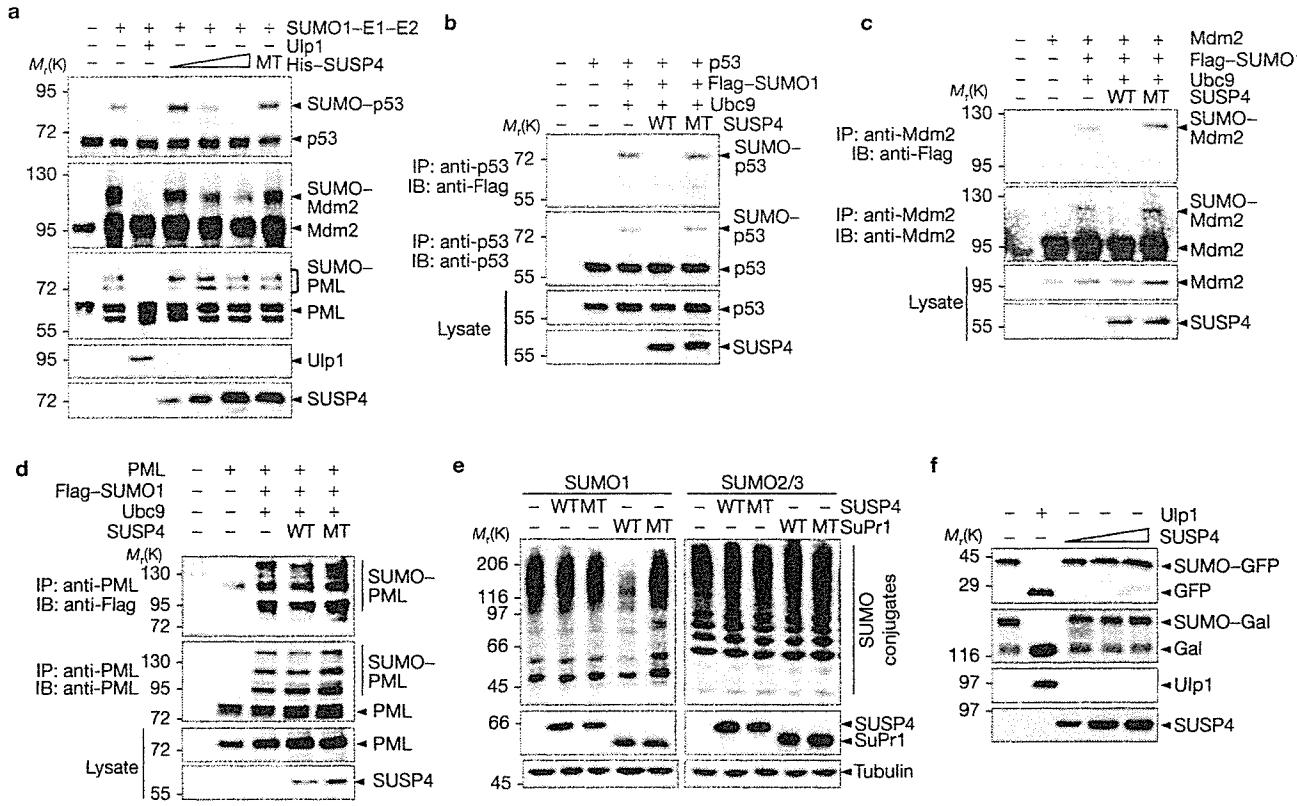

Figure 2 Desumoylation of p53 and Mdm2 by SUSP4. (**a**) *In vitro*-translated Myc–p53, HA–Mdm2 and PML were sumoylated and immunoprecipitated with their antibodies. The samples were incubated for 2 h at 37 °C with or without partially purified SUSP4 (0.05, 0.1 and 0.2 μg), SUSP4^{C460S} (0.2 μg) or Ulp1 (0.1 μg). After incubation, the samples were subjected to SDS–PAGE followed by immunoblot analysis. Ulp1 and SUSP4 were probed with their antibodies. (**b–d**) pcDNA–Myc–p53 (**b**), pcDNA–HA–Mdm2 (**c**) or pcDNA–HA–PML (**d**) were transfected into HEK293T cells with pcDNA–HisMax–SUSP4 (wild type; WT) or pcDNA–HisMax–SUSP4^{C460S} (mutant; MT). Cells were also transfected with pSG5–Flag–SUMO-1 and pCMV2–Flag–Ubc9. After incubation for 36 h, sumoylated proteins were subjected to immunoprecipitation followed by immunoblot analysis. (**e**) NIH3T3 cells were transfected with pCMV2–Flag–SUSP4 (WT) or pCMV2–Flag–SUSP4^{C460S} (MT) or with pCMV2–Flag–SuPr1 (WT) or pCMV2–Flag–SuPr1^{C466S} (MT). After incubation for 36 h, cell lysates were immunoblotted with anti-SUMO-1 or anti-SUMO-2 and -3 antibody. (**f**) SUMO–GFP and SUMO–β-Gal were incubated with Ulp1 (0.1 μg) or SUSP4 (0.05, 0.1 and 0.2 μg) at 37 °C for 2 h. After incubation, the samples were immunoblotted with anti-GFP or anti-β-Gal antibodies.

C-terminal regions of Mdm2 and p53, respectively. These results suggest that SUSP4 and p53 may compete with each other for binding to the same N-terminal region of Mdm2.

To determine whether SUSP4 shows desumoylating activity, *in vitro*-translated p53, Mdm2 and PML (promyelocytic leukaemia protein) were sumoylated and incubated with SUSP4 or Ulp1. SUSP4 removed SUMO-1 from p53 and Mdm2, but not from PML, p63, p73 or RanGAP1 (Fig. 2a and data not shown). Although SUSP4^{C460S} could not release SUMO-1 from any of the substrates, Ulp1 could desumoylate all of them. SUSP4 also showed desumoylating activity under *in vivo* conditions towards p53 (Fig. 2b) and Mdm2 (Fig. 2c), whereas SUSP4^{C460S} did not. Neither SUSP4 nor SUSP4^{C460S} acted on PML, p63, p73 or RanGAP1 *in vivo* (Fig. 2d and data not shown). We then examined whether SUSP4 overexpression may cause nonspecific cleavage of cellular proteins modified by endogenous SUMO-1 or its isoforms. SUSP4 showed little or no activity towards cellular proteins modified by SUMO-1, -2 or -3, whereas SuPr1 showed strong desumoylating activity only towards SUMO-1-modified proteins (Fig. 2e). Neither SUSP4^{C460S} nor SuPr1^{C466S}, in which the active site Cys 466 was replaced by Ser, acted on any of the SUMO conjugates. Thus, SUSP4 seems to specifically act on SUMO-1-modified p53 and Mdm2. SUMO-1 is synthesized in cells as a precursor protein with an extension of several amino acids at its C-terminus. To determine whether SUSP4 can process the SUMO-1 precursor, SUMO-1–GFP and SUMO-1–β-galactosidase were incubated with SUSP4. Neither of the linear fusions was cleaved by SUSP4, whereas both were hydrolysed by Ulp1 (Fig. 2f). In addition, SUSP4 could not cleave a mouse SUMO-1 precursor containing the C-terminal extension of His–Ser–Thr–Val (data not shown). These results suggest that SUSP4 acts only SUMO-1 molecules attached to target proteins.

Mdm2 is a ubiquitin ligase that targets itself, as well as p53. To determine whether sumoylation of Mdm2 influences its activity, p53, Mdm2 and His–ubiquitin were overexpressed in *p53*$^{-/-}$*mdm2*$^{-/-}$ MEF cells with SUSP4 or SUSP4^{C460S}. SUSP4, but not SUSP4^{C460S}, caused an increase in Mdm2 ubiquitination in parallel with a decrease in p53 ubiquitination (Fig. 3a). These results raised the possibility that SUMO modification influences Mdm2 in a manner that switches the ubiquitin ligase activity from Mdm2 to p53. To examine this possibility, Mdm2 and sumoylated Mdm2 were isolated and incubated with p53 and fluorescein-labelled ubiquitin. The ability of sumoylated Mdm2 to self-ubiquitinate was much lower than that of unmodified Mdm2 (Fig. 3b), indicating that SUMO modification attenuates the self-ubiquitinating activity of Mdm2. In contrast, sumoylated Mdm2 could ubiquitinate p53 better than unmodified Mdm2. Thus, it seems that the sumoylation status of Mdm2 is important in controlling the switch between

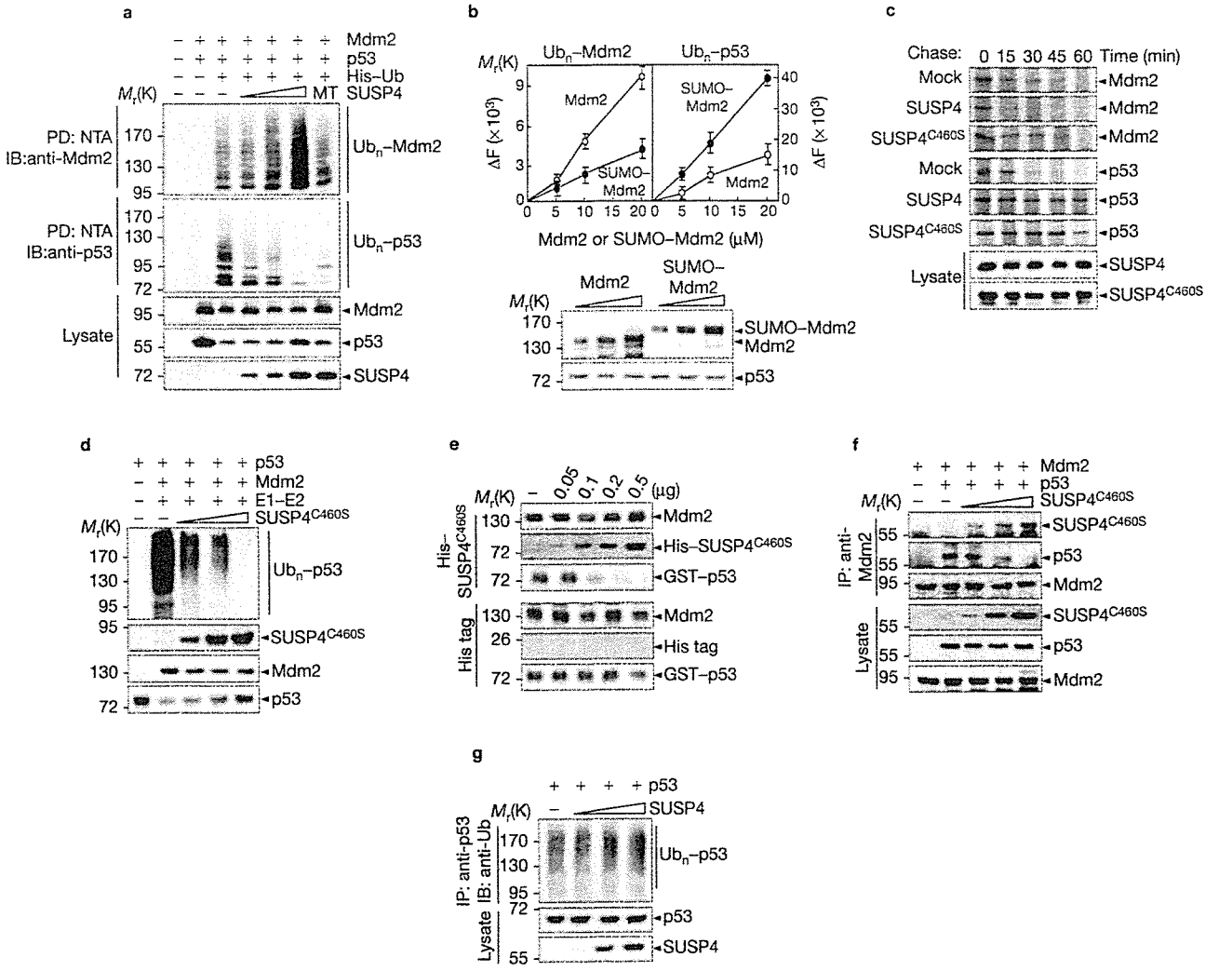

Figure 3 Effect of SUSP4 on ubiquitination and stability of Mdm2 and p53. (**a**) pcDNA–Myc–p53, pcDNA–HA–Mdm2 and pcDNA–HisMax–ubiquitin (Ub) were transfected to *p53*$^{-/-}$*mdm2*$^{-/-}$ cells with pCMV2–Flag–SUSP4 (2, 4 and 8 μg) or pCMV2–Flag–SUSP4^{C460S} (8 μg). After incubation for 4 h with 10 μM MG132, ubiquitinated proteins were pulled down by NTA resins and subjected to immunoblot analysis with anti-Mdm2 or anti-p53 antibodies. Uncropped images of the upper two panels are shown in the Supplementary Information, Fig. S5a. (**b**) MBP–Mdm2, Sae1–Sae2 and Ubc9 were incubated with or without SUMO-1. Mdm2 and sumoylated Mdm2 were separated using a DEAE–Sepharose column and each was incubated with p53, fluorescein-N-terminal ubiquitin, Uba1, UbcH5 and an ATP-regenerating system for 1 h. The reaction was stopped by adding 150 mM Tris–HCl (pH 7.6) containing 5% SDS and 30% glycerol. The mixtures were immunoprecipitated by anti-Mdm2 or anti-p53 antibodies and the precipitates were quantified using a fluorometer. The same amounts of the input p53, Mdm2 and SUMO–Mdm2 proteins were subjected to SDS–PAGE and Coomassie stained. The data represent the mean ± s.d. of three experiments. (**c**) NIH3T3 cells transfected with an empty vector (Mock), pCMV2–Flag–SUSP4 or pCMV2–Flag–SUSP4^{C460S} were labelled with ^{35}S-methionine followed by treatment with unlabelled methionine. The labelled proteins were subjected to immunoprecipitation with anti-Mdm2 or anti-p53 antibodies followed by SDS–PAGE, and visualized by autoradiography. (**d**) Mdm2 (0.1 μg) was incubated with SUSP4^{C460S} (0.1, 0.2 and 0.5 μg) for 30 min at 4 °C. The samples were subjected to *in vitro* ubiquitination followed by immunoprecipitation with anti-p53 antibodies. They were then immunoblotted with anti-ubiquitin antibodies. (**e**) Mdm2 (0.5 μg) was incubated with His–SUSP4^{C460S} or His-tag itself for 30 min and then with purified GST–p53 (0.2 μg) for 1 h. The samples were subjected to immunoprecipitation with anti-Mdm2 antibodies. (**f**) pcDNA–Mdm2 (1 μg) and pcDNA–Myc–p53 (1 μg) were transfected to *p53*$^{-/-}$*mdm2*$^{-/-}$ cells with pCMV2–Flag–SUSP4^{C460S} (0.5, 1 and 2 μg). After culturing for 24 h, cell lysates were subjected to immunoprecipitation with anti-Mdm2 antibodies followed by immunoblot with anti-Flag, anti-p53 or anti-Mdm2 antibodies. (**g**) *p53*$^{-/-}$*mdm2*$^{-/-}$ cells were transfected with pcDNA–Myc–p53 and pCMV2–Flag–SUSP4. After incubation as in **a**, cell lysates were subjected to immunoprecipitation with anti-p53 antibodies and probed with anti-ubiquitin antibodies.

self-ubiquitination and p53 ubiquitination. Furthermore, pulse-chase analysis using ^{35}S-methionine reveals that SUSP4, but not SUSP4^{C460S}, causes a marked decrease in Mdm2 stability (Fig. 3c). SUSP4 also caused p53 stabilization. These results indicate that SUSP4 destabilizes Mdm2 by promoting its self-ubiquitinating activity, thereby leading to p53 stabilization.

Surprisingly, however, expression of SUSP4^{C460S}, which cannot desumoylate Mdm2, caused a marked decrease in the level of ubiquitinated p53 (Fig. 3a). Moreover, SUSP4^{C460S}, which showed little or no effect on Mdm2 stability, caused p53 stabilization (Fig. 3c). We showed that SUSP4 binds to the N-terminal region of Mdm2 (see Supplementary Information, Fig. S3). The binding site of p53 has also been identified to reside within the N-terminal region of Mdm2 (ref. 29). Thus, it seemed possible that competition between SUSP4^{C460S} and p53 for binding to Mdm2 results in p53 stabilization. To investigate this possibility, we first examined whether SUSP4^{C460S} can block p53 ubiquitination by Mdm2 *in vitro*. The level of ubiquitinated p53 was decreased by SUSP4^{C460S}

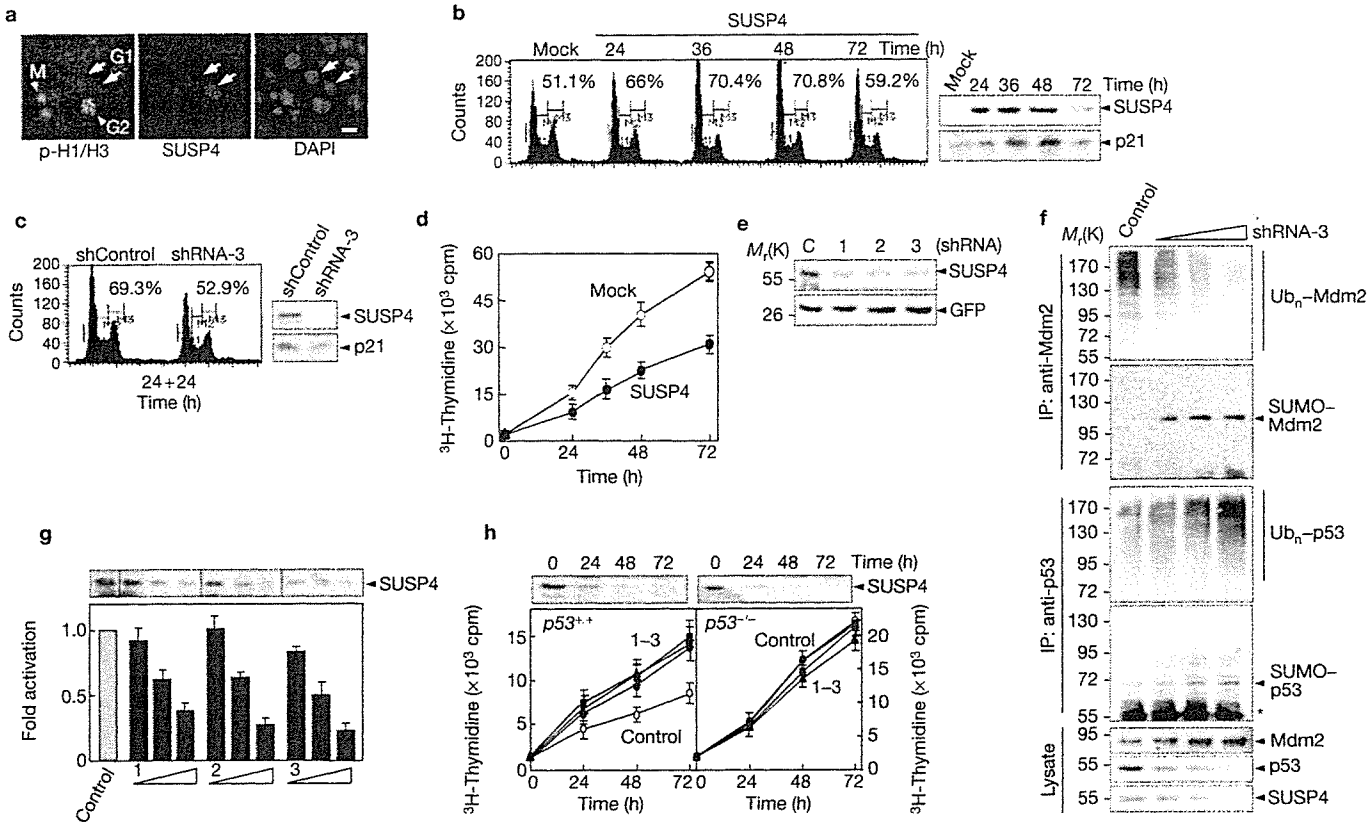

Figure 4 SUSP4-mediated inhibition of cell growth. (**a**) NIH3T3 cells were transiently transfected with pCMV–Myc–SUSP4. After incubation for 24 h, cells were stained with anti-Myc or a mixture of anti-phospho-histone H1 and H3 antibodies. The scale bar represents 10 μm. (**b**) Cells transfected with pCMV2–Flag–SUSP4 or an empty vector (Mock) were cultured for the indicated times and subjected to FACS analysis to determine their DNA content. They were also subjected to immunoblot analysis with anti-SUSP4 or anti-p21 antibodies. The data represents the mean ± s.d. of three experiments. (**c**) Cells transfected with pCMV2–Flag–SUSP4 were incubated for 24 h. After incubation, they were transfected with control shRNA (shControl) or shRNA-3 and cultured for a further 24 h. FACS and immunoblot analyses were then performed as in **b**. (**d**) Cells cultured as in **b** were assayed for ^{3}H-thymidine incorporation. (**e**) Each of three shRNAs (1–3) or control shRNA (C) was transfected for two rounds into cells with a vector encoding GFP as a transfection control. After incubation for 24 h, cells were subjected to immunoblot analysis with anti-SUSP4 or anti-GFP antibodies. (**f**) Cells transfected with increasing amounts of shRNA-3 were subjected to immunoprecipitation with anti-Mdm2 or anti-p53 antibodies followed by immunoblot with anti-ubiquitin or anti-SUMO-1 antibodies. Uncropped images of the second and fourth panels are shown in the Supplementary Information, Fig. S5b. The asterisk indicates the IgG heavy chain. (**g**) Control shRNA or increasing amounts of shRNAs (1–3) were transfected to cells with pG13–Luc and pcDNA–β-Gal. After incubation for 24 h, cells were subjected to luciferase assay. Data represents mean ± s.d. of three experiments. Cell lysates were also subjected to immunoblot with anti-SUSP4 antibodies. (**h**) *p53*$^{+/+}$ and *p53*$^{-/-}$ cells were transfected with control shRNA or shRNAs (1–3). They were then assayed for ^{3}H-thymidine incorporation. The level of SUSP4 was determined in cells transfected with shRNA-3 by immunoblot with anti-SUSP4 antibodies. The data represents the mean ± s.d. of three experiments. Uncropped images of the upper panels are shown in the Supplementary Information, Fig. S5c.

treatment in a dose-dependent manner (Fig. 3d), indicating that SUSP4^{C160S} is capable of inhibiting Mdm2-mediated p53 ubiquitination. We then examined whether SUSP4^{C160S} actually competes with p53 for binding to Mdm2. Purified Mdm2 was incubated with increasing amounts of His–SUSP4^{C160S} and then with p53. Immunoprecipitation analysis using anti-Mdm2 antibodies revealed that the amount of SUSP4^{C160S} bound to Mdm2 gradually increased in parallel with a decrease in the amount of p53 bound to Mdm2 (Fig. 3e). *In vivo* competition experiments were also performed. Mdm2 and p53 were expressed in *p53*$^{-/-}$*mdm2*$^{-/-}$ cells with increasing amounts of SUSP4^{C160S}. The amount of SUSP4^{C160S} coprecipitated with Mdm2 increased in parallel with a decrease in the amount of p53 coprecipitated with Mdm2 (Fig. 3f). Nearly identical results were obtained with wild-type SUSP4 in both *in vivo* and *in vitro* competition experiments (data not shown). These results indicate that both SUSP4 and SUSP4^{C160S} are capable of competing with p53 for binding to Mdm2.

As SUSP4 can also desumoylate p53, we examined the effect of SUSP4 on p53 ubiquitination under conditions where Mdm2 is absent by expressing p53 with increasing amounts of SUSP4 in *p53*$^{-/-}$*mdm2*$^{-/-}$ cells. In contrast with the results obtained in the presence of Mdm2 (see Fig. 3a), SUSP4 showed little or no effect on p53 ubiquitination in the absence of Mdm2 (Fig. 3g). These results indicate that the effects of SUSP4 on the stability of p53, as well as of Mdm2, are mediated by its action on Mdm2 but not on p53. Taken together, these results suggest that SUSP4 can stabilize p53 in two different modes: by interfering with the interaction between p53 and Mdm2; and by promoting self-ubiquitination and destabilization of Mdm2 through desumoylation of Mdm2.

As SUSP4 increased p53 stability, we examined the effect of SUSP4 on p53 transcriptional activity when NIH3T3 cells were transfected with reporter vectors. SUSP4 caused a marked increase in the activity of both endogenous and ectopically expressed p53 (see Supplementary Information, Fig. S4a). Immunoblot analysis of the same cell lysates again showed that SUSP4

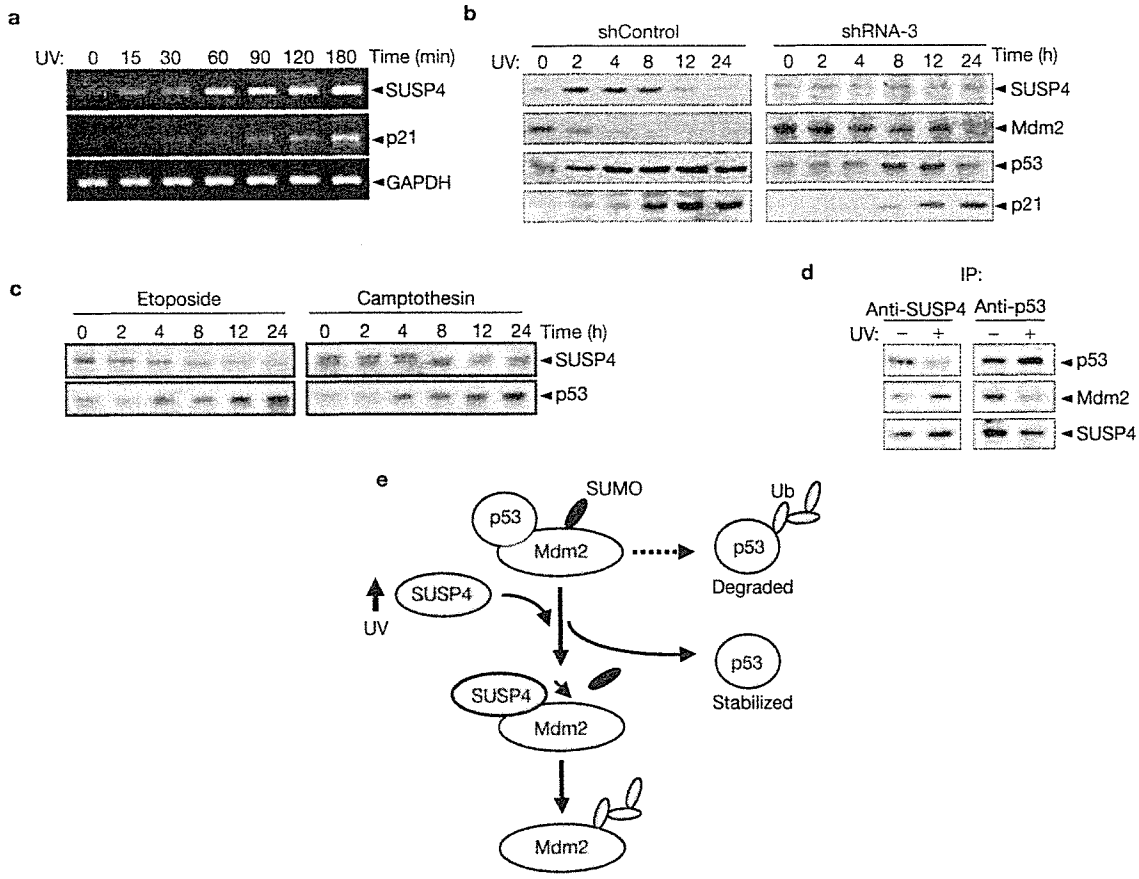

Figure 5 Induction of SUSP4 expression by UV. (**a**) NIH3T3 cells were irradiated with UV (50 J m^{-2}) for 30 s and incubated for the indicated times. Total RNAs were prepared from cells using Triazol reagent. RT–PCR was then carried out using specific primers for *susp4*, *p21* and *GAPDH*. (**b**) Cells were transfected with control shRNA or shRNA-3 for two rounds. After incubation for 24 h, cells were irradiated with UV. They were then subjected to immunoblot with respective antibodies. (**c**) Cells were treated with 20 μM etoposide or 10 μg ml^{-1} of camptothesin, and incubated for the indicated times. They were then subjected to immunoblot with anti-SUSP4 or anti-p53 antibody. (**d**) Cells that had been treated without (–) or with UV (+) were incubated for 1 h. After incubation, cells were subjected to immunoprecipitation with anti-SUSP4 or anti-p53 antibody followed by immunoblot with respective antibodies. Uncropped images of the left upper two panels and the right lower two panels are shown in the Supplementary Information, Fig. 5Sd. (**e**) A schematic representation of a model for SUSP4-mediated control of the p53–Mdm2 pathway by SUSP4

stabilizes p53. $SUSP4^{C460S}$ also increased the stability and activity of p53. However, SUSP4 had little or no effect on the stability and activity of p50 (NF-κB; see Supplementary Information, Fig. S4b). These results suggest that both SUSP4 and $SUSP4^{C460S}$ positively regulate p53 activity by antagonizing endogenous Mdm2. These results also suggest that the SUSP4-mediated increase in p53 activity is independent of p53 sumoylation. To confirm this, p53 or $p53^{K386R}$ (in which the SUMO-accepting Lys residue was replaced by Arg) were expressed in cells with SUSP4. SUSP4 caused a marked increase in the stability and activity of both p53 and $p53^{K386R}$ (see Supplementary Information, Fig. S4c). Thus, it seems that p53 sumoylation itself has little or no influence on the SUSP4-mediated increase in p53 activity.

We then examined the effect of SUSP4 on the stability and activity of p53 in conditions where Mdm2 was overproduced. As expected, Mdm2 expression resulted in a dramatic reduction in p53 activity by destabilizing it (see Supplementary Information, Fig. S4d). Coexpression of SUSP4 or $SUSP4^{C460S}$ reversed the Mdm2-mediated decrease in p53 activity. On the other hand, neither SuPr1 nor $SuPr1^{C466S}$ could stabilize p53 or reverse the Mdm2-mediated decrease in p53 activity, indicating that Mdm2 is a specific target of SUSP4. Moreover, Mdm2 expression resulted in a marked reduction in *p21* mRNA levels, but coexpression of SUSP4 or $SUSP4^{C460S}$ reversed the inhibitory effect of Mdm2 (see Supplementary Information, Fig. S4e). Little or no accumulation of *p21* mRNA was observed on expression of NF-κB, regardless of whether SUSP4 or $SUSP4^{C460S}$ was coexpressed. These results further demonstrate that SUSP4 positively regulates p53 activity by antagonizing Mdm2 function.

As SUSP4 mediates p53 stabilization, we examined whether SUSP4 is involved in p53-dependent control of cell growth. NIH3T3 cells transfected with pCMV–Myc–SUSP4 were strongly stained by anti-Myc antibodies (Fig. 4a). However, the same cells were barely stained by a mixture of anti-phospho-histone H1 and H3 antibodies, which is a characteristic feature of G1-phase cells. These results suggest that SUSP4 overexpression leads to cell-cycle arrest at the G1 phase. To confirm this, cells transfected with pCMV2–Flag–SUSP4 were cultured for various times and subjected to FACS analysis to determine their DNA contents. The fraction of cells in G1 phase was significantly increased up to 48 h in culture (Fig. 4b). The level of p21 protein was also gradually increased up to 48 h in culture. Both the fraction of G1-phase cells and p21 levels decreased thereafter, most likely due to an increase in the number of cells that were not transfected with pCMV2–Flag–SUSP4, as SUSP4 levels also decreased at 72 h. Furthermore, cotransfection of a *susp4*-specific short hairpin RNA (shRNA-3; see below), but not a negative control vector (shControl), resulted in a decrease in both the fraction of cells in the G1 phase and p21

levels (Fig. 4c), indicating that shRNA-3 can reverse the cell-cycle arrest caused by SUSP4 overexpression. We then examined whether SUSP4-mediated cell-cycle arrest leads to inhibition of cell growth. The rate of ^{3}H-thymidine incorporation was significantly reduced by transfection of cells with pCMV2–Flag–SUSP4 compared with that of an empty vector (Fig. 4d). Taken together, these results suggest that overproduced SUSP4 can downregulate the growth of cells by stabilizing p53.

To clarify the involvement of SUSP4 in p53-mediated control of cell growth, three *susp4*-specific shRNAs (indicated by 1–3) were transfected into NIH3T3 cells with a vector encoding GFP. All three shRNAs effectively reduced endogenous SUSP4 levels (Fig. 4e). Therefore, we examined the effect of shRNA-3 on ubiquitin and SUMO-1 modification of Mdm2. shRNA-mediated knockdown of *susp4* caused a decrease in the level of ubiquitinated Mdm2 in parallel with an increase in the level of sumoylated Mdm2, leading to stabilization of endogenous Mdm2 and destabilization of endogenous p53 (Fig. 4f). Consistently, all three shRNAs caused a decrease in the transcriptional activity of endogenous p53 in a dose-dependent manner (Fig. 4g). Moreover, the rate of ^{3}H-thymidine incorporation was significantly increased by transfection of $p53^{+/+}$ cells with the shRNAs, compared with that observed with the control shRNA (Fig. 4h), indicating that SUSP4 is involved in downregulation of cell growth. In contrast, knockdown of *susp4* had little or no effect on the proliferation of $p53^{-/-}$ cells (Fig. 4h), demonstrating the link between p53 and SUSP4 in the control of cell growth. Taken together, these results reveal that SUSP4 has an important function in the control of cell growth by p53.

Given that UV damage is one of the major stresses that provokes p53 action, we examined whether UV induces *susp4* gene transcription. *susp4* mRNA levels dramatically increased as early as 15 min after UV irradiation (Fig. 5a). *p21* mRNA level also increased about 1 h after the irradiation. These results suggest that SUSP4 is an UV-inducible protein that stabilizes p53, leading to an increase in *p21* mRNA levels. To determine whether UV-induced SUSP4 influences the endogenous levels of Mdm2 and p53 proteins, NIH3T3 cells transfected with control shRNA or shRNA-3 was irradiated with UV. Concurrent with an increase in SUSP4 levels, Mdm2 levels were sharply declined in cells transfected with control shRNA (Fig. 5b). p53 levels then gradually increased, followed by an increase in endogenous p21 levels. On the other hand, shRNA-mediated knockdown of *susp4* resulted in a marked delay in the accumulation of p53 and p21. These results indicate that SUSP4 has a critical role in the control of the cellular levels of Mdm2 and consequently of p53 and p21, when cells are damaged by UV. However, etoposide and camptothesin, which also cause DNA damage, showed little or no effect on SUSP4 induction (Fig. 5c), suggesting that SUSP4 responds to a limited range of stresses, such as UV.

We then examined whether UV damage causes an alteration in the amounts of p53 and Mdm2 that bind to SUSP4. UV irradiation led to an increase in the amount of Mdm2 bound to SUSP4, with a decrease in the interaction between p53 and SUSP4 (Fig. 5d). UV also caused a decrease in the amounts of SUSP4 and Mdm2 that bind to p53. These results suggest that UV damage leads to an increase in relative abundance of the SUSP4–Mdm2 complex over p53–Mdm2 complex through competition of accumulated SUSP4 with p53 for binding to Mdm2.

Mdm2 targets not only p53, but also itself for ubiquitination, and the fate of p53 is determined accordingly. Recently, Daxx (a multifunctional protein involved in the control of apoptosis and transcription) was shown to have a key role in switching the Mdm2 activity from p53 to itself in response to DNA damage[30]. Here, we have provided an additional mechanism for the control of Mdm2 function and a model for the involvement of SUSP4 in the control of the p53–Mdm2 pathway, based on the results obtained in this study, is shown in Figure 5d. On UV damage, SUSP4 accumulates and replaces p53 for binding to Mdm2, leading to stabilization of p53 for induction of cell-cycle arrest and cell-growth inhibition. Desumoylation by SUSP4 would then promote self-ubiquitination and degradation of Mdm2 for further stabilization of p53. However, under normal conditions (that is, when SUSP4 levels are low), the SUMO-modification system, including Ubc9, may override SUSP4 and sumoylate Mdm2, leading to promotion of p53 ubiquitination. Thus, SUSP4 seems to have a critical role in switching the Mdm2 activity from p53 to itself in response to UV damage. □

METHODS

Plasmids and antibodies. *susp4* cDNA was isolated from a mouse brain cDNA library and cloned into pcDNA–Myc, pcDNA–HisMax, pCMV–Myc and pCMV2–Flag. It was also cloned into pET-32a for bacterial expression. Therefore, His–SUSP4 and His-tag itself contain an extra-amino acid sequence of approximately 20K corresponding to the multicloning site region of the vector. *susp4*-specific shRNAs were synthesized and cloned into pSilencer 2.0-U6 (Ambion, Austin, TX). Oligonucelotides used were: 1, GATCAGGGATGGTATTTAA; 2, GATGAGGTCATCAATTTCT; 3, GAATGTTTACCTGTAAAT.

Antibodies against Myc (9E10), SUMO-1 (D-11), p53 (DO-1 and N-19), p50 (H-119), p21 (C-19) and Mdm2 (SMT4) were obtained from SantaCruz (Santa Cruz, CA). Peroxidase-conjugated AffiniPure goat anti-rabbit and anti-mouse, and donkey anti-goat IgGs, FITC-conjugated goat anti-rabbit IgG, and TRITC-conjugated goat anti-mouse IgG were purchased from Jackson ImmunoResearch Laboratories (West Glove, PA). Anti-Flag M2, anti-Xpress, anti-Ub (FK1; Affiniti Res, Manhead, UK), and anti-SUMO-2 and -3 (Zymed, San Francisco, CA) antibodies were also used. Rabbit polyclonal anti-SUSP4 antiserum was raised against a recombinant His-tagged N-terminal fragment of SUSP4 (that is, amino acids 1–320). Anti-SUSP4 IgGs were purified by applying the serum onto an affinity column, which had been generated by conjugation of the N-terminal SUSP4 fragments to NHS-activated Sepharose 4 Fast Flow. Anti-SUSP4 IgGs bound to the resins were eluted with 100 mM glycine buffer (pH 3.0).

Cell culture and transfection. HEK293T, NIH3T3, MEF cells ($p53^{+/+}$, $p53^{-/-}$, and $p53^{-/-}mdm2^{-/-}$) were grown at 37 °C in DMEM) supplemented with 100 units ml^{-1} penicillin, 1 μg ml^{-1} streptomycin and 10% FBS. Transfections in HEK293T and NIH3T3 cells were carried out using LipofectaminePlus. MEF cells were transfected by electroporation.

Immunocytochemistry. NIH3T3 cells plated on gelatin-coated cover-glasses were fixed with 2% formaldehyde in PBS for 30 min at room temperature and permeabilized with 0.5% Triton X-100 in PBS. All subsequent dilutions and washes were performed with PBS containing 0.1% Triton X-100 (PBS-T). Nonspecific binding sites were saturated by incubation for 30 min with a blocking solution consisting of 10% goat serum, 1% BSA and 1% gelatin in PBS. Cells were incubated with primary antibody for 1 h and washed with PBS-T four times at 10 min intervals. They were then incubated with FITC- or TRITC-conjugated secondary antibody for 1 h and washed four times. DAPI was used for counterstaining the nuclei. The cover glasses were mounted in Vectashield and cells were visualized under a Zeiss Axioplan II microscope.

Assays for protein–protein interaction. Cells were lysed in buffer A consisting of 50 mM Tris–HCl (pH 7.4), 120 mM NaCl, 0.5% NP40 and 1× protease inhibitor cocktail. Cell lysates were incubated with appropriate antibodies for 2 h at 4 °C and then with 50 μl of a 50% slurry of protein A–Sepharose for 1 h. The resins were collected by centrifugation and washed five times with buffer B consisting of 20 mM Tris–HCl (pH 7.4), 500 mM NaCl, 1 mM EDTA and 0.5% NP40. Bound proteins were eluted by boiling in 0.2% SDS and subjected to SDS–PAGE followed by immunoblot with appropriate antibodies.

To analyse the competition of SUSP4^{C460S} with p53 for binding to Mdm2 *in vitro*, Mdm2-affinity resins were prepared by incubation of 0.5 μg of purified Mdm2 for 2 h at 4 °C with protein A–Sepharose that had been treated with anti-Mdm2 antibody. The resins were incubated with increasing amounts of His–SUSP4^{C460S} for 30 min at 4 °C and then with 0.2 μg of GST–p53 for the next 1 h. The resins were washed three times with buffer A to remove SUSP4^{C460S} and p53 that did not bind to Mdm2. Proteins bound to the resins were then eluted by boiling in 0.2% SDS and subjected to SDS–PAGE.

Assays for sumoylation and desumoylation. For *in vitro* assays, *in vitro*-translated Myc–p53, HA–Mdm2 and PML were prepared by using TNT-coupled reticulocyte lysate systems. The resulting proteins were sumoylated by incubation with 10 μg of purified SUMO-1, 1.5 μg of Sae1–Sae2, 2 μg of Ubc9, an ATP-regenerating system (50 mM Tris–HCl at pH 7.5, 5 mM $MgCl_2$, 10 mM creatine phosphate, 5 units ml^{-1} of phosphocreatine kinase and 5 mM ATP), and 1× protease inhibitor cocktail. After incubation, SUMO-modified proteins were immunoprecipitated with anti-p53, anti-Mdm2 or anti-PML antibody followed by washing with PBS containing 500 units ml^{-1} of apyrase and 1 mM *N*-ethylmaleimide and then with 2 mM DTT. The substrates were then incubated at 37 °C for 2 h with recombinant His-tagged SUSP4 or SUSP4^{C460S}. After incubation, the samples were subjected to SDS–PAGE on 8% gels followed by immunoblot with the same antibodies.

For *in vivo* assays, Myc–p53, Flag–SUMO-1 and Flag–Ubc9 were expressed in HEK293T cells with or without HisMax–SUSP4. HA–Mdm2 or HA–PML were also expressed in cells as above. After culturing for 36 h, cells were lysed by boiling for 10 min in 150 mM Tris–HCl (pH 6.7) buffer containing 5% SDS and 30% glycerol. Cell lysates were diluted twentyfold with buffer A containing 1× protease inhibitor cocktail, incubated with appropriate antibodies for 2 h at 4 °C and treated with protein-A–Sepharose[31]. To assay sumoylation by endogenous SUMO-1, NIH3T3 cells that had been transfected with *susp4*-specific shRNAs were cultured for 36 h and then treated as above. The resins were collected by centrifugation and washed five times with buffer B. The samples were then subjected to SDS–PAGE followed by immunoblot analysis.

^{3}H-Thymidine incorporation. NIH3T3 and MEF cells (2×10^1 cells per well) were seeded in 12-well plates and grown for various periods. They were then cultured in serum-free media for 2 h and treated with ^{3}H-thymidine (1 μCi per well). After incubation for 6 h, cells were subjected to trichloroacetic acid extraction followed by scintillation counting.

Flow cytometry. NIH3T3 cells were transfected with an empty vector or pCMV2–Flag–SUSP4 in 60-mm dishes. After incubation, cells were harvested and washed twice with PBS. They were fixed by treatment with 1 ml of 70% ethanol, gently vortexed and kept at 4 °C until used. Fixed cells were washed once with PBS and resuspended in a propidium iodide solution (10 μg ml^{-1}) containing 4% NP40 and RNase A (250 μg ml^{-1}). Propidium iodide-stained cells were then analysed for their DNA contents by using a FACS instrument (BD Biosciences, Franklin Lakes, CA).

Pulse-chase analysis. NIH3T3 cells that had been transfected with appropriate vectors were cultured for 18 h. Cells were divided into four fractions and further cultured on 60-mm dishes for 12 h. They were then incubated with 100 μCi ml^{-1} of ^{35}S-methionine in methione-free DMEM for 30 min at 37 °C. After incubation, cells were washed twice with PBS and further incubated in DMEM supplemented with 10% FBS and 2 mM unlabelled methionine for various periods. Cell lysates prepared in buffer A were subjected to immunoprecipitation with anti-p53 or anti-Mdm2 antibodies, followed by SDS–PAGE. Gels were then fixed, dried and visualized by autoradiography.

Accession numbers The GenBank accession number for *susp4* cDNA is AF366264.

Note: Supplementary Information is available on the Nature Cell Biology website.

ACKNOWLEDGEMENTS

We thank G. Lozano and H. Kim for providing *p53*$^{-/-}$ *mdm2*$^{-/-}$ and *p53*$^{-/-}$ MEF cells. We also thank R. Hay for providing pGEX–Sae1–Sae2. This work was supported by grants from the Korea Science and Engineering Foundation (M10533010001-05N3301-00100) and the Korea Research Foundation (KRF-2003-070-C00033 and KRF-2005-084-C00025).

COMPETING FINANCIAL INTERESTS

The authors declare that they have no competing financial interests.

Published online at http://www.nature.com/naturecellbiology/
Reprints and permissions information is available online at http://npg.nature.com/reprintsandpermissions/

1. Ko, L. J. & Prives, C. p53: puzzle and paradigm. *Genes Dev.* **10,** 1054–1072 (1996).
2. Vogelstein, B., Lane, D. & Levine, A. J. Surfing the p53 network. *Nature* **408,** 307–310 (2000).
3. Haupt, Y., Maya, R., Kazaz, A. & Oren, M. Mdm2 promotes the rapid degradation of p53. *Nature* **387,** 296–299 (1997).
4. Kubbutat, M. H., Jones, S. N. & Vousden, K. H. Regulation of p53 stability by Mdm2. *Nature* **387,** 299–303 (1997).
5. Li, M. *et al.* Mono- versus polyubiquitination: differential control of p53 fate by Mdm2. *Science* **302,** 1972–1975 (2003).
6. Melchior, F. SUMO — nonclassical ubiquitin. *Annu. Rev. Cell Dev. Biol.* **16,** 591–626 (2000).
7. Muller, S., Hoege, C., Pyrowolakis, G. & Jentsch, S. SUMO, ubiquitin's mysterious cousin. *Nature Rev. Mol. Cell Biol.* **2,** 202–210 (2001).
8. Pichler, A., Gast, A., Seeler, J. S., Dejean, A. & Melchior, F. The nucleoporin RanBP2 has SUMO1 E3 ligase activity. *Cell* **108,** 109–120 (2002).
9. Kagey, M. H., Melhuish, T. A. & Wotton, D. The polycomb protein Pc2 is a SUMO E3. *Cell* **113,** 127–137 (2003).
10. Kahyo, T., Nishida, T. & Yasuda, H. Involvement of PIAS1 in the sumoylation of tumor suppressor p53. *Mol. Cell* **8,** 713–718 (2001).
11. Sachdev, S. *et al.* PIASy, a nuclear matrix-associated SUMO E3 ligase, represses LEF1 activity by sequestration into nuclear bodies. *Genes Dev.* **15,** 3088–3103 (2001).
12. Kim, K. I. *et al.* A new SUMO-1-specific protease, SUSP1, that is highly expressed in reproductive organs. *J. Biol. Chem.* **275,** 14102–14106 (2000).
13. Melchior, F., Schergaut, M. & Pichler, A. SUMO: ligases, isopeptidases and nuclear pores. *Trends Biochem. Sci.* **28,** 612–618 (2003).
14. Hay, R. T. SUMO: a history of modification. *Mol. Cell* **18,** 1–12 (2005).
15. Li, S. J. & Hochstrasser, M. A new protease required for cell-cycle progression in yeast. *Nature* **398,** 246–251 (1999).
16. Li, S. J. & Hochstrasser, M. The yeast *ULP2* (*SMT4*) gene encodes a novel protease specific for the ubiquitin-like Smt3 protein. *Mol. Cell Biol.* **20,** 2367–2377 (2000).
17. Yeh, E. T., Gong, L. & Kamitani, T. Ubiquitin-like proteins: new wines in new bottles. *Gene* **248,** 1–14 (2000).
18. Gong, L. & Yeh, E. T. Characterization of a family of nucleolar SUMO-specific proteases with preference for SUMO-2 or SUMO-3. *J. Biol. Chem.* **281,** 15869–15877 (2006).
19. Gostissa, M. *et al.* Activation of p53 by conjugation to the ubiquitin-like protein SUMO-1. *EMBO J.* **18,** 6462–6471 (1999).
20. Rodriguez, M. S. *et al.* SUMO-1 modification activates the transcriptional response of p53. *EMBO J.* **18,** 6455–5461 (1999).
21. Muller, S. *et al.* c-Jun and p53 activity is modulated by SUMO-1 modification. *J. Biol. Chem.* **275,** 13321–13329 (2000).
22. Kwek, S. S., Derry, J., Tyner, A. L., Shen, Z. & Gudkov, A. V. Functional analysis and intracellular localization of p53 modified by SUMO-1. *Oncogene* **20,** 2587–2599 (2001).
23. Schmidt, D. & Muller, S. Members of the PIAS family act as SUMO ligases for c-Jun and p53 and repress p53 activity. *Proc. Natl Acad. Sci. USA* **99,** 2872–2877 (2002).
24. Xirodimas, D. P., Chisholm, J., Desterro, J. M., Lane, D. P. & Hay, R. T. P14ARF promotes accumulation of SUMO-1 conjugated (H)Mdm2. *FEBS Lett.* **528,** 207–211 (2002).
25. Chen, L. & Chen, J. MDM2–ARF complex regulates p53 sumoylation. *Oncogene* **22,** 5348–5357 (2003).
26. Boggio, R., Colombo, R., Hay, R. T., Draetta, G. F. & Chiocca, S. A mechanism for inhibiting the SUMO pathway. *Mol. Cell* **16,** 549–561 (2004).
27. Tago, K., Chiocca, S. & Sherr, C. J. Sumoylation induced by the Arf tumor suppressor: a p53-independent function. *Proc. Natl Acad. Sci. USA* **102,** 7689–7694 (2005).
28. Best, J. L. *et al.* SUMO-1 protease-1 regulates gene transcription through PML. *Mol. Cell* **10,** 843–855 (2002).
29. Chen, J., Marechal, V. & Levine, A. J. Mapping of the p53 and mdm-2 interaction domains. *Mol. Cell Biol.* **13,** 4107–4114 (1993).
30. Tang, J. *et al.* Critical role for Daxx in regulating Mdm2. *Nature Cell Biol.* **8,** 855–862 (2006).
31. Goodson, M. L. *et al.* Sumo-1 modification regulates the DNA binding activity of heat shock transcription factor 2, a promyelocytic leukemia nuclear body associated transcription factor. *J. Biol. Chem.* **276,** 18513–18518 (2001).

nature
cell biology

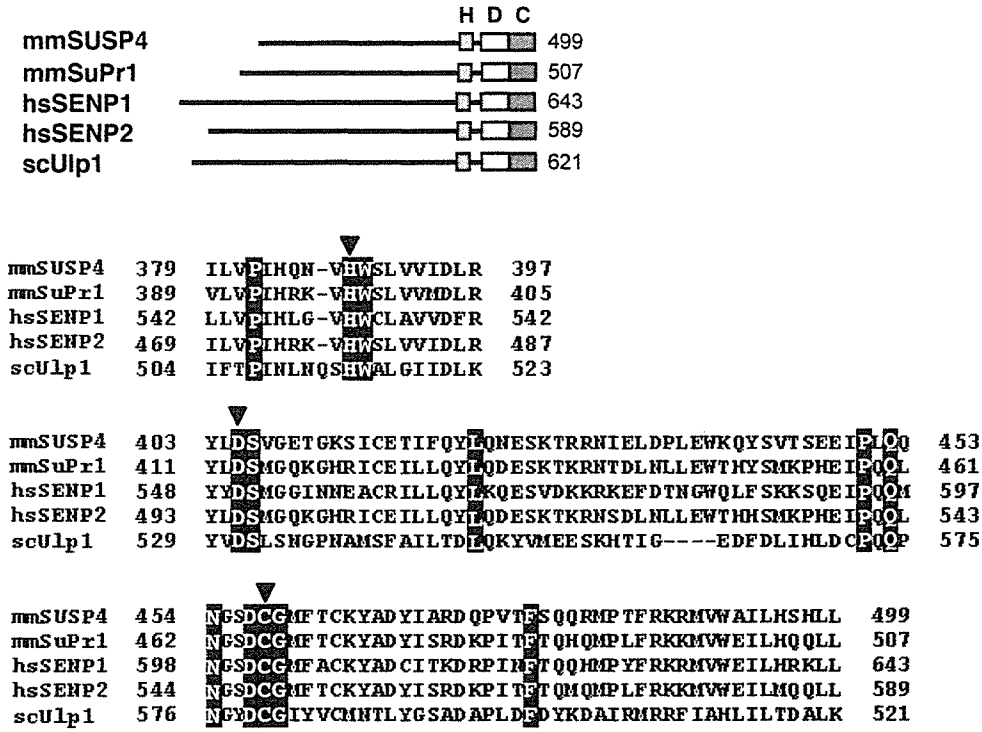

Figure S1 Sequence of SUSP4. Schematic diagrams compares the primary structure of mouse SUSP4 with that of other SUMO-specific proteases. The boxes denote the conserved domains carrying the His-Asp-Cys catalytic triad (upper). The sequences of conserved active site domains of SUSP4 were compared with those of other SUMO proteases. The catalytic residues were indicated by the triangles, and the invariant residues were shaded (lower).

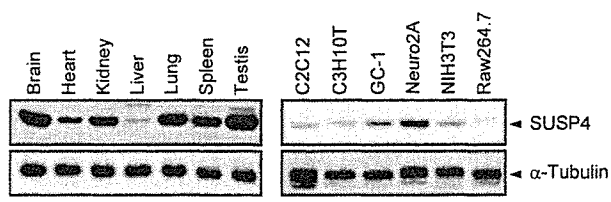

Figure S2 Expression of SUSP4 in various tissues and cell lines. Extracts were prepared from various mouse tissues and cell lines. Aliquots of them (50 μg) were then subjected to SDS-PAGE followed by immunoblot with anti-SUSP4 or anti-α-tubulin antibody.

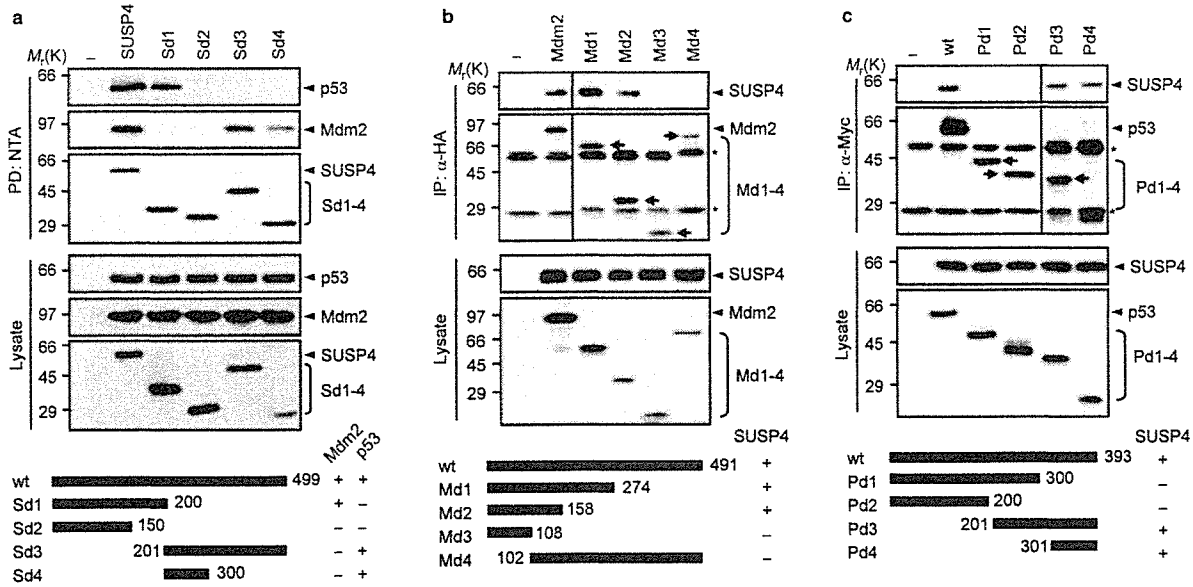

Figure S3 Mapping of binding regions within SUSP4, p53, and Mdm2. (**a**) pcDNA-p53 and pcDNA-Mdm2 were co-transfected to HEK293T cells with pcDNA-HisMax-SUSP4 or vectors expressing SUSP4 deletion mutants (Sd1-Sd4). His-tagged proteins were pulled down (PD) by treatment with NTA resins and subjected to immunoblot with anti-p53, anti-Mdm2, or anti-Xpress antibody. The abilities of SUSP4 and its deletions to interact with p53 and Mdm2 were shown as "+" or "–". (**b**) pCMV2-Flag-SUSP4 was transfected to cells with pcDNA-HA-Mdm2 or vectors expressing Mdm2 deletions (Md1-Md4). Cell lysates were subjected to immunoprecipitation with anti-HA antibody followed by immunoblot with anti-Flag or anti-HA antibody. The asterisks indicate the IgG heavy and light chains, and the arrows show the deletion mutants. The abilities of Mdm2 and its deletions to interact with SUSP4 were shown as "+" or "–". (**c**) pCMV2-Flag-SUSP4 was transfected to cells with pcDNA-Myc-p53 or the vectors expressing p53 deletions (Pd1-Pd4). Cell lysates were subjected to immunoprecipitation with anti-Myc antibody followed by immunoblot with anti-Flag or anti-Myc antibody. The abilities of p53 and its deletions to interact with SUSP4 were shown as "+" or "–".

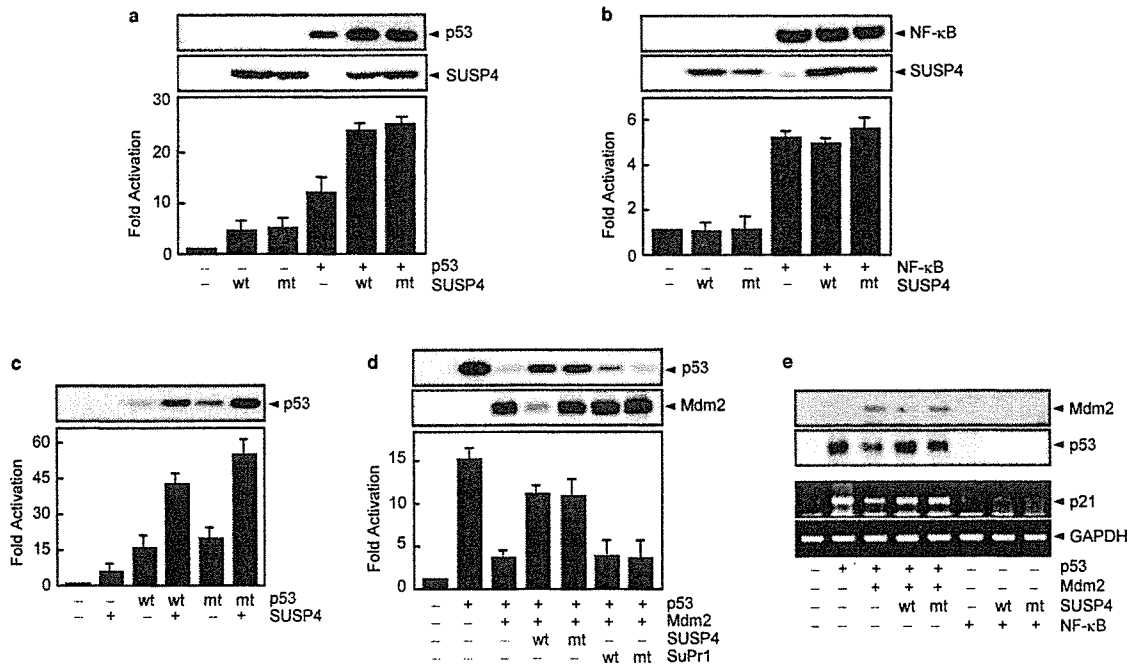

Figure S4 SUSP4-mediated promotion of p53 transcriptional activity. (**a**) pG13-Luc and pcDNA-β-Gal reporter vectors were transfected to NIH3T3 cells with indicated combinations of pCMV2-Flag-SUSP4 (wt), pCMV2-Flag-SUSP4-C460S (mt), and pcDNA-Myc-p53. Cell lysates were subjected to immunoblot analysis and luciferase assay. The luciferase activities seen with transfection of the indicated vectors were expressed as relative folds to the activity seen with transfection of empty vectors after normalization with β-galactosidase activity. Total amounts of transfected DNA were kept constant by supplementing proper amounts of empty vectors. Data represents mean (SD of triplicates. (**b-d**) Experiments were performed as in **a**, but using different combinations of the vectors. In **b**, pGL2-Luc and pcDNA-p50 were used in place of pG13-Luc and pcDNA-Myc-p53. In **c**, both pcDNA-Myc-p53 (wt) and pcDNA-Myc-p53-K386R (mt) were used. In **d**, pcDNA-Mdm2, pCMV2-Flag-SuPr1 (wt), and pCMV2-Flag-SuPr1-C466S (mt) were also used. (**e**) NIH3T3 cells were transfected with the indicated combinations of pcDNA-Myc-p53, pcDNA-Mdm2, pcDNA-p50, and pCMV2-Flag-SUSP4 (wt) or pCMV2-Flag-SUSP4-C460S (mt). Cell lysates were immunoblotted with anti-p53 or anti-Mdm2 antibody (upper). Total RNAs were extracted from the cells using Trizol reagent (Invitrogen), and subjected to real-time RT-PCR using specific primers for p21 and GAPDH (lower).

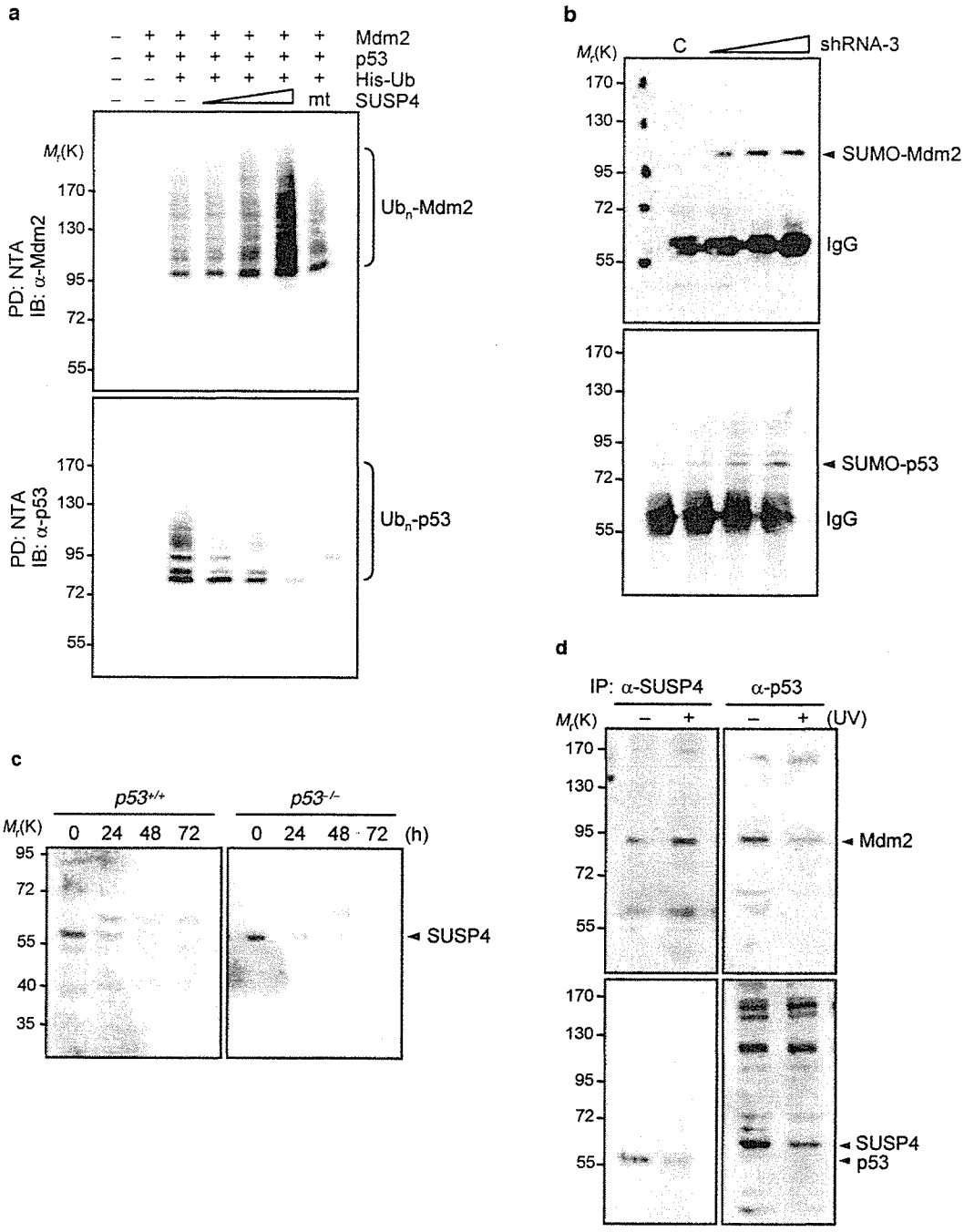

Figure S5 (**a**) Full scans of the upper two panels of Fig. 3a. (**b**) Full scans of the second and fourth panels of Fig. 4f. (**c**) Full scans of the upper panels of Fig. 4h. (**d**) Full scans of the left upper two panels and the right lower two panels in Fig. 5d.

Molecular Cell 24, 977–984, December 28, 2006 ©2006 Elsevier Inc. DOI 10.1016/j.molcel.2006.11.015

Short Article

Cooperation of Multiple Chaperones Required for the Assembly of Mammalian 20S Proteasomes

Yuko Hirano,[1] Hidemi Hayashi,[2,4] Shun-ichiro Iemura,[5] Klavs B. Hendil,[6] Shin-ichiro Niwa,[4] Toshihiko Kishimoto,[2,3] Masanori Kasahara,[7] Tohru Natsume,[5] Keiji Tanaka,[1] and Shigeo Murata[1,8,*]

[1]Laboratory of Frontier Science
Core Technology and Research Center
Tokyo Metropolitan Institute of Medical Science
Bunkyo-ku, Tokyo 113-8613
[2]Proteome Analysis Center
[3]Department of Biomolecular Science
Faculty of Science
Toho University
Funabashi, Chiba 274-8510
[4]Link Genomics, Inc.
Chuo-ku, Tokyo 103-0024
[5]National Institute of Advanced Industrial Science and Technology
Biological Information Research Center
Kohtoh-ku, Tokyo 135-0064
Japan
[6]Institute of Molecular Biology and Physiology
University of Copenhagen
13 Universitetsparken
DK 2100 Copenhagen
Denmark
[7]Department of Pathology
Hokkaido University Graduate School of Medicine
Sapporo, Hokkaido 060-8638
[8]PRESTO
Japan Science and Technology Agency
Kawaguchi, Saitama 332-0012
Japan

Summary

The 20S proteasome is a catalytic core of the 26S proteasome, a central enzyme in the degradation of ubiquitin-conjugated proteins. It is composed of 14 distinct gene products that form four stacked rings of seven subunits each, $\alpha_{1-7}\beta_{1-7}\beta_{1-7}\alpha_{1-7}$. It is reported that the biogenesis of mammalian 20S proteasomes is assisted by proteasome-specific chaperones, named PAC1, PAC2, and hUmp1, but the details are still unknown. Here, we report the identification of a chaperone, designated PAC3, as a component of α rings. Although it can intrinsically bind directly to both α and β subunits, PAC3 dissociates before the formation of half-proteasomes, a process coupled with the recruitment of β subunits and hUmp1. Knockdown of PAC3 impaired α ring formation. Further, PAC1/2/3 triple knockdown resulted in the accumulation of disorganized half-proteasomes that are incompetent for dimerization. Our results describe a cooperative system of multiple chaperones involved in the correct assembly of mammalian 20S proteasomes.

*Correspondence: smurata@rinshoken.or.jp

Introduction

The ubiquitin-proteasome system is the main nonlysosomal route for intracellular protein degradation in eukaryotes. Short-lived proteins as well as abnormal proteins are recognized by the ubiquitin system and are marked with ubiquitin chains as degradation signals. Polyubiquitinated proteins are then recognized and degraded by 26S proteasomes. The 26S proteasome is composed of one proteolytically active 20S proteasome and two 19S regulatory particles, each attached to one end of the 20S proteasome. The 20S proteasome is a barrel-shaped complex made of two outer α rings and two inner β rings that is a conserved architecture in eukaryotes (Groll et al., 1997, 2005; Unno et al., 2002). The α and β rings are each made up of seven structurally similar subunits, of the α or β type, respectively. The proteolytic activity is exerted by three of the β subunits, namely β1, β2, and β5, which are synthesized in an inactive precursor form and whose propeptides are removed to allow the formation of active sites, accompanied by the assembly of 20S proteasomes.

Our previous work indicated that the assembly of mammalian 20S proteasomes is an ordered multistep process, starting from α ring formation with the help of proteasome-specific chaperones named PAC1 (proteasome assembling chaperone 1) and PAC2 (Hirano et al., 2005). The PAC1-PAC2 heterodimer binds to early α subunit assembly intermediates that contain a restricted subset of α subunits and promotes the formation of heteroheptameric α rings. Moreover, PAC1-PAC2 is responsible for suppressing the formation of off-pathway, nonproductive α ring dimers and thus is important for efficient half-proteasome formation (Hirano et al., 2005). Mammalian half-proteasomes are composed of seven α subunits, seven β subunits, some of which are in precursor forms, and proteasome-dedicated chaperones such as hUmp1 (POMP, Proteassemblin, a homolog of yeast Ump1) (Burri et al., 2000; Griffin et al., 2000; Ramos et al., 1998; Witt et al., 2000) and PAC1-PAC2 (Hirano et al., 2005). Lastly, dimerization of the two half-proteasomes occurs with the help of hUmp1, which completes the maturation of 20S proteasomes, with removal of propeptides of β subunits followed by degradation of hUmp1 and the PAC1-PAC2 heterodimer (Chen and Hochstrasser, 1996; De et al., 2003; Heinemeyer et al., 2004; Hirano et al., 2005; Kingsbury et al., 2000; Nandi et al., 1997; Ramos et al., 1998; Schmidtke et al., 1996). However, the mechanism responsible for half-proteasome formation after the assembly of α rings, i.e., how β subunits and hUmp1 are assembled on α rings, remains elusive. We speculated that another chaperone might be involved in this step.

Results and Discussion

Identification of PAC3 as a Component of α Rings

To identify molecules that are potentially involved in 20S proteasome maturation, we purified α rings from HEK293T cells stably expressing Flag-PAC1 and analyzed them

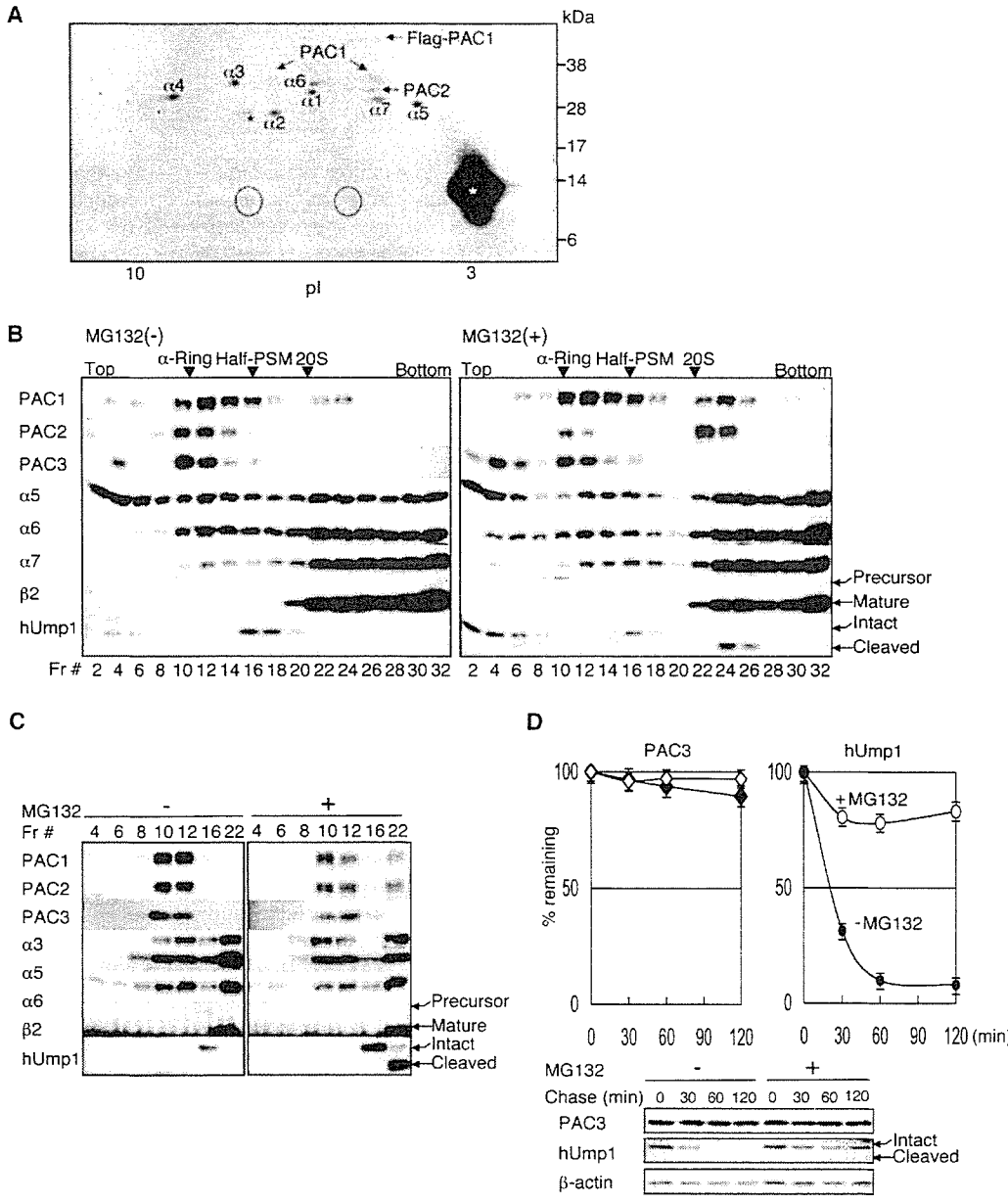

Figure 1. Identification of PAC3 as a Component of α Rings

(A) 2D-PAGE and CBB staining of purified α rings. The α rings were purified from HEK293T cells stably expressing Flag-PAC1 by glycerol gradient centrifugation followed by immunoprecipitation of α ring fractions with M2 agarose. All the spots were identified by MS/MS. The two spots indicated by circles represent hypothetical protein MGC10911. Asterisks indicate nonspecific spots.

(B) 4%–24% glycerol gradient centrifugation of the extracts of HEK293T cells treated with or without MG132. Fractions were immunoblotted as indicated. Arrowheads depict the locations of subcomplexes of proteasomes. Half-PSM, half-proteasomes; 20S, 20S proteasomes. Note that 26S proteasomes sediment near the bottom fraction.

(C) Fractions from (B) were immunoprecipitated with anti-α6 antibody, followed by immunoblotting.

(D) The half-life of PAC3 and hUmp1. Cycloheximide was added to HEK293T cells pretreated with or without 20 μM MG132 for 20 min, and the cells were chased for the indicated time points in the presence or absence of MG132, respectively. The cell lysates were subjected to immunoblotting for PAC3, hUmp1, and β-actin (loading control, bottom). The decay curves of PAC3 (top, left) and hUmp1 (top, right) were generated from the band quantification of the bottom panels. Data are mean ± SEM values of three independent experiments.

by two-dimensional polyacrylamide gel electrophoresis (2D-PAGE). In addition to the spots of α subunits and PAC1-PAC2 heterodimer, we found two spots of ~14 kDa. Using tandem mass spectrometry (MS/MS), we identified the two spots as a protein called MGC10911 (Figure 1A). We renamed it PAC3 (for proteasome assembling chaperone-3). PAC3 is a small protein of 122 amino acids with no distinct domains or homology to any other known proteins, and its function was entirely unknown. We found genes with significant similarity in metazoans, plants, and fungi, as for PAC2, PAC3, and hUmp1, but in metazoans and fungi as for PAC1 (Figure S1 in the Supplemental Data available with this article online).

First, to examine the behavior of endogenous PAC3, extracts from HEK293T cells were separated by glycerol

gradient centrifugation. PAC3 was located in the α ring fractions (fractions 10–12), i.e., in fractions without β subunits but with α subunits and PAC1-PAC2 (Figure 1B, left). The association of PAC3 with α subunits and PAC1-PAC2 was confirmed by immunoprecipitation with anti-α6 antibody followed by immunoblotting, indicating that PAC3 is a component of α rings, similar to PAC1-PAC2 (Figure 1C, left). Interestingly, when the cells were treated with a proteasome inhibitor, MG132, PAC3 was increased in the light fractions (fractions 2–6), whereas PAC1-PAC2 accumulated in the 20S proteasome fractions (fractions 22–24) as reported previously by our group (Figure 1B, right panels) (Hirano et al., 2005). This suggests that PAC3 dissociates from precursor proteasomes during the maturation pathway, unlike PAC1-PAC2 and hUmp1 (Hirano et al., 2005; Ramos et al., 1998). The increase in PAC3 in the light fractions does not represent an increase in newly synthesized PAC3 upon MG132 treatment, because PAC3 messenger RNA was not increased at this point of time (data not shown). To examine whether the stability of PAC3 is also regulated differently from that of PAC1-PAC2 and hUmp1, which have been shown to be short-lived proteins (Hirano et al., 2005; Ramos et al., 1998), we measured the half-life of PAC3 as well as that of hUmp1 by determining the protein levels at various time points after treatment with cycloheximide. As shown in Figure 1D, hUmp1 had a short half-life of about 20 min, which was greatly prolonged by MG132. This observation is consistent with the previous report (Ramos et al., 1998). As for hUmp1, we noted accumulation of its free forms (Figure 1B, right, fractions 2–6) as well as its cleaved forms in 20S proteasome fractions upon MG132 treatment (Figures 1B–1D). In contrast, PAC3 had a much longer half-life, which was not affected by MG132. These results suggest that PAC3 is involved in the maturation of 20S proteasomes and behaves differently from PAC1-PAC2 and hUmp1.

Knockdown of PAC3 Attenuates α Ring Formation

To elucidate the role of PAC3 in the assembly of the 20S proteasome in vivo, we performed small interfering RNA (siRNA)-mediated knockdown of PAC3 as well as PAC1+PAC2 (PAC1/2), PAC1+PAC2+PAC3 (PAC1/2/3), and hUmp1 to specify their distinct roles. In PAC3 knockdown cells, where we achieved a 75% reduction of PAC3 mRNA (data not shown), polyubiquitin-conjugated proteins accumulated to a level comparable to that in PAC1/2 knockdown cells (Figure 2A). In PAC1/2/3 knockdown cells, the accumulation of polyubiquitinated proteins was enhanced, and the effect of such knockdown was as large as with hUmp1 knockdown (Figure 2A). Consistent with these observations, the decrease in chymotrypsin-like activity of proteasomes was comparable between PAC3 and PAC1/2 knockdown, and the activity was profoundly reduced in PAC1/2/3 knockdown, similar to that in hUmp1 knockdown. These results suggest that PAC1-PAC2 and PAC3 are not epistatic with each other but rather work differently or compensate each other.

To determine the role of PAC3 in the assembly of 20S proteasomes, extracts of knockdown cells were subjected to glycerol gradient analysis (Figure 2C and Figure S2). To compare the quantity of relevant components in each fraction, fractions corresponding to α ring, half-proteasome, and 20S proteasomes in each knockdown experiment were electrophoresed in the same gel (Figure 2D). PAC1/2 knockdown resulted in reduction of α ring peak and emergence of α ring dimers in the half-proteasome fractions (fractions 14–16) as we reported previously (Hirano et al., 2005), and it turned out that PAC3 was a component of this abnormal structure (Figure 2C, bottom left, and Figure 2D, lane 7), indicating that PAC3 plays no role in inhibiting the formation of α ring dimers. The accumulation of PAC3 in light fractions (Figure 2C, bottom left, fractions 4–6) was probably due to ineffective α ring formation in PAC1/2 knockdown cells. Ectopic expression of PAC3 in PAC1/2 knockdown cells did not complement the phenotypes in regard to the formation of α ring dimers and reduction in proteasome activity (Figure S3), indicating that PAC3 and PAC1-PAC2 play distinct roles in α ring formation and do not function redundantly.

In PAC3 knockdown cells, we also observed a reduction of the α ring peak, but no α ring dimers (Figure 2C, top right). Consequently, half-proteasomes, which included α subunits, pro-β subunits, and hUmp1 in proportions like those observed in control cells, were formed to a lesser extent, resulting in decreased formation of 20S proteasomes (Figure 2D, lanes 8 and 13). In addition, PAC1-PAC2 accumulated in light fractions, and free forms of α subunits were increased in PAC3 knockdown cells as well as PAC1/2 and PAC1/2/3 knockdown cells (Figure 2C, top right, and Figure S4). These results suggest that PAC3 plays an important role in α ring assembly and that poor α ring formation resulted in surplus PAC1-PAC2 heterodimer and free α subunits in light fractions.

Simultaneous Loss of PAC1-PAC2 and PAC3 Causes Accumulation of Disorganized Half-Proteasomes

Intriguingly, in PAC1/2/3 knockdown cells, several α subunits and β subunits, including pro-β2 and hUmp1, cosedimented in the half-proteasome fractions to levels comparable to, or even higher (for example, hUmp1, pro-β1, and pro-β2) than, those in control cells, but still the formation of 20S proteasomes was severely impaired (Figure 2C, bottom right, and Figure 2D, lanes 9 and 14). Specifically, the amount of pro-β5, whose propeptide is essential for 20S proteasome formation in yeast (Chen and Hochstrasser, 1996), was much smaller in the complex observed in the half-proteasome fraction of PAC1/2/3 knockdown cells than control cells (Figure 2D, lanes 6 and 9, and Figure 2E). Considering that α ring formation is attenuated by knockdown of both PAC1/2 and PAC3, these results suggest that this complex of abnormal half-proteasomes, observed in PAC1/2/3 knockdown cells, accumulated because it could not dimerize to form mature 20S proteasomes, at least due to a shortage of pro-β5, which should accompany a disorganized constitution of this abnormal half-proteasomes.

Taken together, the knockdown experiments suggest that both PAC1-PAC2 and PAC3 contribute to α ring formation by separate mechanisms, and thus, the effects of knockdowns are additive. In addition, our results suggest that PAC1-PAC2 and PAC3 act cooperatively on the correct formation of half-proteasomes. On the other hand, knockdown of hUmp1 did not influence

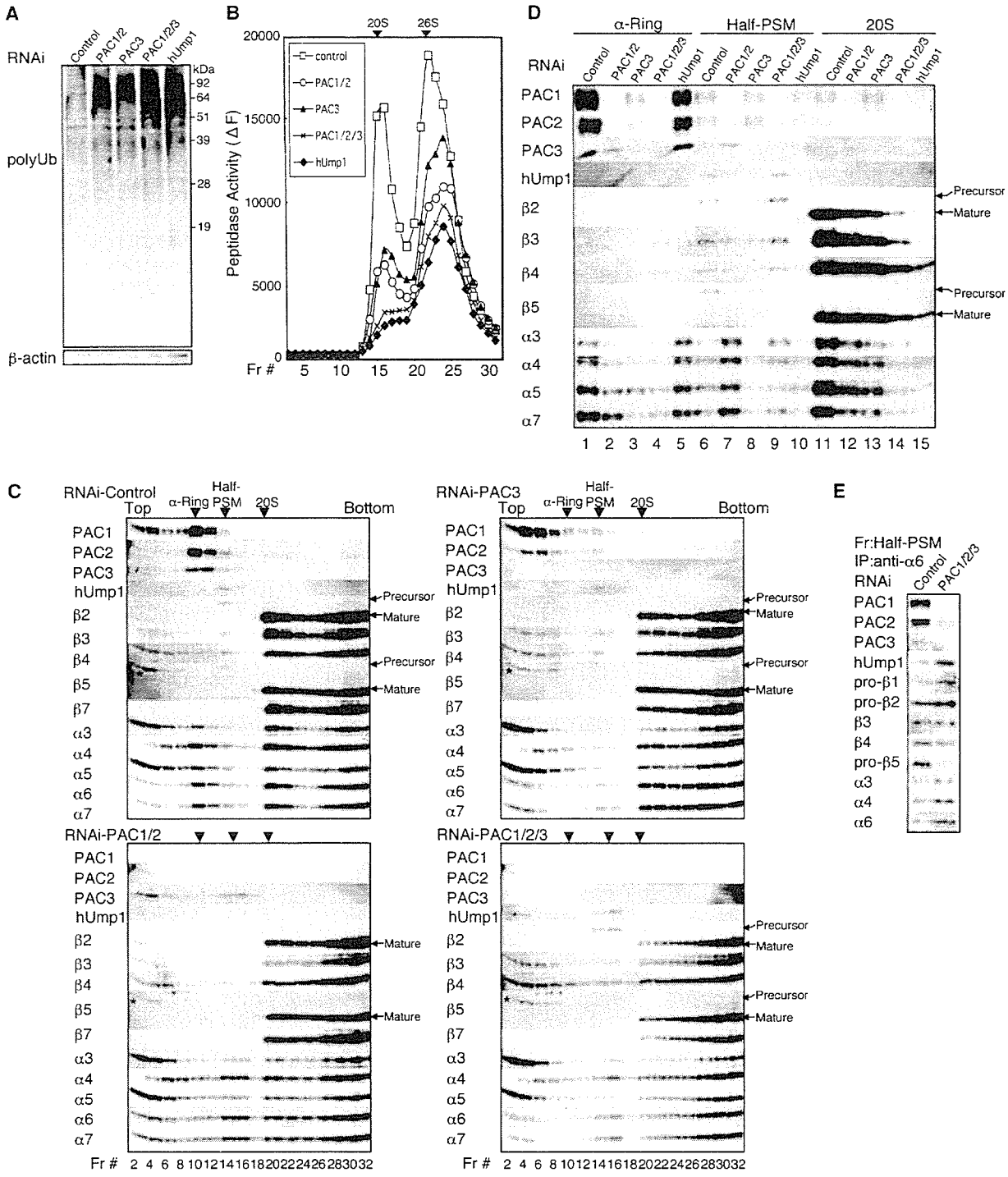

Figure 2. siRNA-Mediated Knockdown of PAC3 Causes Defect in Proteasome Assembly

siRNAs targeting PAC1/2, PAC3, PAC1/2/3, hUmp1, or control were transfected into HEK293T cells. The whole-cell extracts (A) and fractions separated by 8%–32% (B) or 4%–24% (C–E) glycerol gradient centrifugation were immunoblotted (A, C, D, and E) or assayed for Suc-LLVY-MCA hydrolyzing activity of proteasomes (B). In (D), the peak fractions of the indicated subcomplexes from (C) (α ring, fraction 12; Half-PSM, fraction 16; and 20S, fraction 22) were subjected to SDS-PAGE in the same gel to compare the quantity of subunits. (E) Fraction 16 of control or PAC1/2/3 knockdown cells from (C) was immunoprecipitated with anti-α6 antibody, followed by immunoblotting. Data are representative of four experiments.

the sedimentation pattern of PAC3 or PAC1-PAC2 (Figure S2), consistent with the notion that hUmp1 is involved in the last step of the assembly, i.e., dimerization of half-proteasomes, and not in α ring and half-proteasome formation (Hirano et al., 2005; Ramos et al., 1998).

PAC3 Directly Associates with Both α and β Subunits

To gain mechanistic insight into the action of PAC3 and the differences between PAC3 and PAC1-PAC2, we set up in vitro binding experiments. First, we examined direct interactions between PACs. PAC3 did not bind to

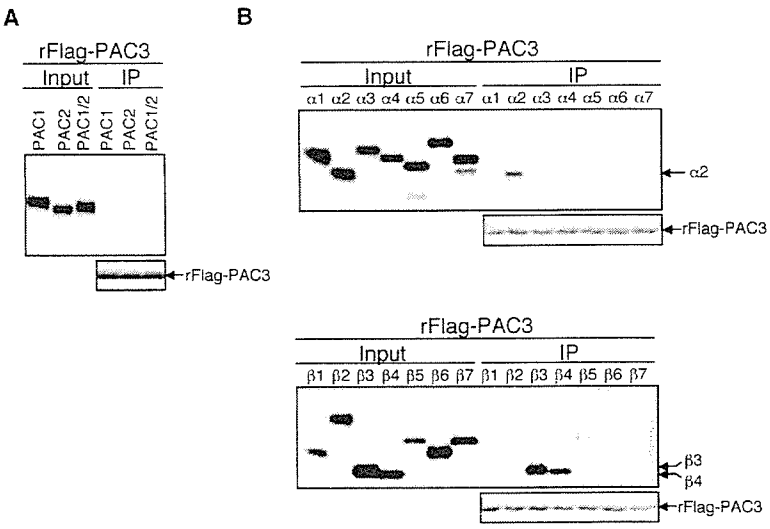

Figure 3. PAC3 Directly Binds to Both α2 and Several β Subunits

(A) Interactions of PAC3 with PAC1 and PAC2. Recombinant Flag-tagged PAC3 (rFlag-PAC3) was incubated with the indicated products translated and radiolabeled in reticulocyte lysates, immunoprecipitated with M2 agarose, and analyzed by SDS-PAGE and autoradiography.

(B) Interactions of PAC3 with individual α and β subunits. Interactions between rFlag-PAC3 and α or β subunits were analyzed as in (A).

PAC1 or PAC2 (Figure 3A). Next, we tested the interactions between PAC3 and each 20S proteasome subunit. PAC3 could directly bind to not only an α subunit (α2) but also to several β subunits, strongly to β3 and β4 but weakly to β1 and β5 (Figure 3B). This is in contrast to the property of PAC1-PAC2, which directly associated with α5 and α7, but not with any of the β subunits (Hirano et al., 2005). These results indicate that PAC1-PAC2 heterodimer and PAC3 are distinct entities that work at different aspects in the maturation of 20S proteasomes.

PAC3 Is Released from Precursor Proteasomes during Half-Proteasome Formation

Because PAC3 seemed to be released from precursor proteasomes during the maturation pathway (Figure 1B), we analyzed the precursor proteasomes that contain PAC3. An extract of HEK293T cells stably expressing Flag-PAC3, -hUmp1, or -PAC1 was separated by glycerol gradient centrifugation, and fractions 8–20, which included α rings (fraction 12) and half-proteasomes (fractions 16–18) were immunoprecipitated with anti-Flag antibody, followed by immunoblotting (Figure 4A). Flag-PAC3 did not precipitate hUmp1 or β subunits in half-proteasome fractions, and Flag-hUmp1 did not precipitate PAC3 at all (Figure 4A). Subsequently, we purified α rings and half-proteasomes from Flag-PAC2 and Flag-hUmp1 expressing cells, respectively, and subjected them to immunoblotting and CBB staining. Although half-proteasomes were loaded in much larger molar amounts, a band corresponding to PAC3, which was clearly visible in α rings, was not observed in half-proteasomes (Figure 4B and Figure S5). These results clearly show that the release of PAC3 from precursor proteasomes is coupled to the recruitment of hUmp1 and β subunits. Considering that PAC3 can directly bind to several β subunits in vitro (Figure 3B) and that PAC3 knockdown together with PAC1/2 knockdown resulted in production of disorganized half-proteasomes that were not competent for 20S proteasome formation (Figure 2), it is suggested that the association between PAC3 and β subunits is either intrinsically unstable in vivo or destabilized upon half-proteasome formation and that the release of PAC3 from precursor proteasomes is an obligatory step for the correct assembly of half-proteasomes by mediating interactions between α rings and β subunits.

Our present work provides a model (Figure 4C) where the chaperone PAC3 assists in the formation of α rings, together with PAC1-PAC2 heterodimer, and mediates correct formation of half-proteasomes in cooperation with PAC1-PAC2. PAC3 itself is then released and recycled in further rounds of proteasome assembly. The unique feature of PAC3 is its ability to interact with various β subunits, raising the possibility that it plays a role in the assembly of β subunits on α rings. In the present model, we emphasize that correct assembly of mammalian 20S proteasomes is achieved by the cooperative actions of multiple proteasome-specific chaperones.

Experimental Procedures

DNA Constructs

The cDNA encoding PAC3 was synthesized from total RNA isolated from HeLa cells using Superscript II (Invitrogen). PCR was carried out on the cDNA by using Phusion DNA polymerase (FINNZYMES). The cDNAs encoding PAC1, PAC2, PAC3, hUmp1, and proteasome α and β subunits were cloned into pcDNA3.1 (Invitrogen) and/or pIRESpuro3 (Clontech). All constructs were confirmed by sequencing. For expression of Flag-fusion protein, the cDNA was subcloned into pET22b (Novgen) in frame with a C-terminal Flag tag. For expression of GST and MBP-fusion proteins, the cDNAs were subcloned into pGEX6P-1 (Amersham) and pMAL (NEB), respectively.

Cell Culture

HEK293T cell lines were cultured in Dulbecco's modified Eagle's medium (Sigma), supplemented with 10% fetal calf serum (FCS), 100 IU/ml penicillin G, and 100 μg/ml streptomycin sulfate (all from Gibco-Invitrogen). Transfections of plasmids into HEK293T cells were performed with Fugene 6 (Roche). To generate stable cell lines, transfected HEK293T cells were selected with 5 μg/ml of puromycin. We used 20 μM MG132 (Peptide Institute) to inhibit proteasome activities for 2 hr before harvest. For cycloheximide-chase experiments, HEK293T cells were treated with 100 μg/ml cycloheximide (Sigma).

Protein Extracts, Immunological Analysis, and Antibodies

Cells were lysed in ice-cold lysis buffer (50 mM Tris-HCl [pH 7.5], 0.5% [v/v] NP-40, and 1 mM dithiothreitol [DTT]) with 2 mM ATP and 5 mM $MgCl_2$, and the extracts were clarified by centrifugation at 20,000 × g for 10 min at 4°C. The supernatants were mixed with

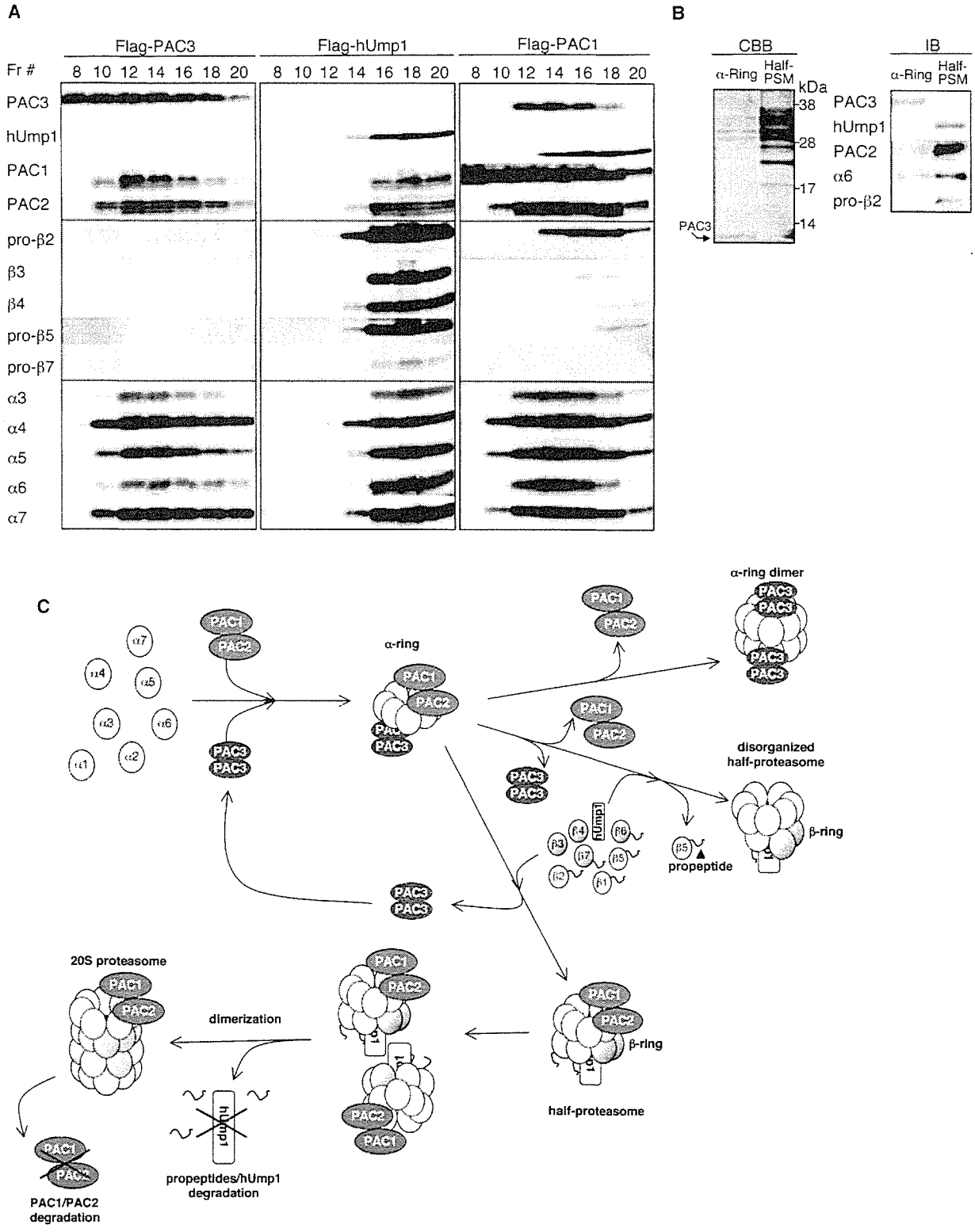

Figure 4. Mutually Exclusive Incorporation of PAC3 and hUmp1 into Precursor Proteasomes

(A) HEK293T cells stably expressing Flag-PAC3, -hUmp1, or -PAC1 were fractionated as in Figure 1B. The indicated fractions were immunoprecipitated with M2 agarose, resolved, and analyzed by SDS-PAGE and immunoblotting.

(B) SDS-PAGE followed by CBB staining (left) and immunoblotting (right) of purified α rings and half-proteasomes. α rings were purified from fraction 12 of Flag-PAC2 expressing cells. Half-proteasomes were purified from fraction 16 of Flag-hUmp1 expressing cells in (A). The band for PAC3 was identified by MS/MS. The 2D-PAGE analyses of these complexes are shown in Figure S5.

(C) A model for proteasome assembly assisted by multiple chaperones. PAC1-PAC2 heterodimer and PAC3, which probably forms homodimers based on the analysis of molecular sieve chromatography of the recombinant PAC3 (data not shown), assist α ring formation. Whereas PAC1-PAC2 suppresses off-pathway aggregation of α subunits and keeps α rings competent for half-proteasome formation, PAC3, which can bind

SDS sample buffer. SDS-PAGE (12% gel or 4%–12% gradient Bis-Tris gel [Invitrogen]) was performed according to the instructions provided by the manufacturer. The separated proteins were transferred onto polyvinylidene difluoride membrane and reacted with the indicated antibody. Development was performed with Western Lighting reagent (PerkinElmer). 2D-PAGE was performed as described previously (Murata et al., 2001).

For immunoprecipitation, we used antibodies MCP20 bound to protein G Sepharose (Amersham) in Figure 1C, antibodies MCP20 crosslinked to NHS-activated Sepharose (Amersham) in Figure 2E, or M2 Agarose (Sigma) in Figures 1A, 4A, and 4B. These beads were added to the extracts, mixed under constant rotation for 2 hr at 4°C, washed four times with lysis buffer with 30 mM NaCl, and boiled in SDS sample buffer. Otherwise, these washed samples were eluted with 100 μg/ml Flag peptides (Sigma) or with 0.2 M glycine-HCl (pH 2.8).

Anti-PAC1 and PAC2 polyclonal antibodies were described previously (Hirano et al., 2005). Anti-PAC3 polyclonal antibodies were raised in rabbits by using recombinant PAC3 (full-length) proteins, which were produced by cleavage of GST by PreScission protease (Amersham) after purification of GST-fused PAC3 proteins. Anti-hUmp1 polyclonal antibodies were raised in rabbits by using recombinant MBP-hUmp1 (full-length) proteins. Antibodies against proteasome α2 subunit (MCP21), α3 (MCP257), α4 (MCP34), α5 (MCP196), α6 (MCP20), α7 (MCP72), β1 (MCP421), β2 (MCP168), β3 (MCP102), and β7 (MCP205) were purchased from BioMol. Anti-β5 (P93250) and β4 (55F8) were prepared as described previously (Tanahashi et al., 2000). Anti-ubiquitin antibodies were obtained from Dako. Anti-β-actin antibodies were from Chemicon.

Glycerol Gradient Analysis

Cell extracts (1 mg of protein) were separated in 32 fractions by centrifugation (22 hr, 100,000 × g) in 4%–24% [v/v] or 8%–32% [v/v] linear gradients, as described previously (Hirano et al., 2005).

Binding Assay

In vitro labeling was performed by using TNT T7 Quick for PCR DNA system (Promega) with ^{35}S-labeled methionine, according to the procedure supplied by the manufacturer. Recombinant Flag-PAC3 proteins were expressed in *E. coli* and purified with M2 Agarose. Binding assay was performed in lysis buffer, and the resulting product was washed with lysis buffer with 150 mM NaCl before elution with Flag peptides. The eluates were separated by SDS-PAGE and visualized by autoradiography.

RNA Interference

siRNA targeting human PAC1, PAC2, PAC3, and hUmp1 with the following 19 nucleotide sequences were designed by B-Bridge and synthesized by Dharmacon. The targeting sequences of PAC1, PAC2, and hUmp1 were described previously (Hirano et al., 2005). These of PAC3 are 5′-CCGUGAAGGACAAAAGCAU-3′ and 5′-GAU CAAUUGUAGGAGGAAA-3′. Control siRNA (Non-specific Control Duplex VIII) was purchased from B-Bridge. Transfections of siRNAs into HEK293T cells were performed by using Lipofectamine 2000 at a final concentration of 50 nM. It was performed three times at intervals of 24 hr. The cells were analyzed 96 hr after first transfection.

Assay of Proteasome Activity

Peptidase activity was measured by using a fluorescent peptide substrate, succinyl-Leu-Leu-Val-Tyr-7-amido-4-methylcoumarin (Suc-LLVY-MCA), as described previously (Murata et al., 2001). Note that the assay was carried out in the presence of 0.03% SDS, which is a potent artificial activator of the latent 20S proteasome, as previously reported (Tanaka et al., 1989).

Supplemental Data

Supplemental Data include five figures and can be found with this article online at http://www.molecule.org/cgi/content/full/24/6/977/DC1/.

Acknowledgments

We thank K. Furuyama for technical support. This work was supported by grants from Japan Science and Technology Agency (to S.M.), the Ministry of Education, Science and Culture of Japan (to S.M. and K.T.), and NEDO (to T.N.). Y.H. was supported by Japan Society for the Promotion of Science.

Received: July 7, 2006
Revised: October 10, 2006
Accepted: November 15, 2006
Published: December 28, 2006

References

Burri, L., Hockendorff, J., Boehm, U., Klamp, T., Dohmen, R.J., and Levy, F. (2000). Identification and characterization of a mammalian protein interacting with 20S proteasome precursors. Proc. Natl. Acad. Sci. USA *97*, 10348–10353.

Chen, P., and Hochstrasser, M. (1996). Autocatalytic subunit processing couples active site formation in the 20S proteasome to completion of assembly. Cell *86*, 961–972.

De, M., Jayarapu, K., Elenich, L., Monaco, J.J., Colbert, R.A., and Griffin, T.A. (2003). β2 subunit propeptides influence cooperative proteasome assembly. J. Biol. Chem. *278*, 6153–6159.

Griffin, T.A., Slack, J.P., McCluskey, T.S., Monaco, J.J., and Colbert, R.A. (2000). Identification of proteassemblin, a mammalian homologue of the yeast protein, Ump1p, that is required for normal proteasome assembly. Mol. Cell Biol. Res. Commun. *3*, 212–217.

Groll, M., Ditzel, L., Lowe, J., Stock, D., Bochtler, M., Bartunik, H.D., and Huber, R. (1997). Structure of 20S proteasome from yeast at 2.4 Å resolution. Nature *386*, 463–471.

Groll, M., Bochtler, M., Brandstetter, H., Clausen, T., and Huber, R. (2005). Molecular machines for protein degradation. ChemBioChem *6*, 222–256.

Heinemeyer, W., Ramos, P.C., and Dohmen, R.J. (2004). The ultimate nanoscale mincer: assembly, structure and active sites of the 20S proteasome core. Cell. Mol. Life Sci. *61*, 1562–1578.

Hirano, Y., Hendil, K.B., Yashiroda, H., Iemura, S., Nagane, R., Hioki, Y., Natsume, T., Tanaka, K., and Murata, S. (2005). A heterodimeric complex that promotes the assembly of mammalian 20S proteasomes. Nature *437*, 1381–1385.

Kingsbury, D.J., Griffin, T.A., and Colbert, R.A. (2000). Novel propeptide function in 20 S proteasome assembly influences β subunit composition. J. Biol. Chem. *275*, 24156–24162.

Murata, S., Udono, H., Tanahashi, N., Hamada, N., Watanabe, K., Adachi, K., Yamano, T., Yui, K., Kobayashi, N., Kasahara, M., et al. (2001). Immunoproteasome assembly and antigen presentation in mice lacking both PA28α and PA28β. EMBO J. *20*, 5898–5907.

Nandi, D., Woodward, E., Ginsburg, D.B., and Monaco, J.J. (1997). Intermediates in the formation of mouse 20S proteasomes: implications for the assembly of precursor β subunits. EMBO J. *16*, 5363–5375.

Ramos, P.C., Hockendorff, J., Johnson, E.S., Varshavsky, A., and Dohmen, R.J. (1998). Ump1p is required for proper maturation of the 20S proteasome and becomes its substrate upon completion of the assembly. Cell *92*, 489–499.

Schmidtke, G., Kraft, R., Kostka, S., Henklein, P., Frommel, C., Lowe, J., Huber, R., Kloetzel, P.M., and Schmidt, M. (1996). Analysis of mammalian 20S proteasome biogenesis: the maturation of β-subunits is an ordered two-step mechanism involving autocatalysis. EMBO J. *15*, 6887–6898.

Tanahashi, N., Murakami, Y., Minami, Y., Shimbara, N., Hendil, K.B., and Tanaka, K. (2000). Hybrid proteasomes. Induction by interferon-γ and contribution to ATP-dependent proteolysis. J. Biol. Chem. *275*, 14336–14345.

directly to several β subunits, dissociates before the formation of half-proteasomes, a process coupled to the recruitment of β subunits and hUmp1. Loss of both PAC1-PAC2 and PAC3 before β subunit incorporation causes formation of disorganized half-proteasomes that lack pro-β5 almost completely. Released PAC3 is recycled. Two half-proteasomes dimerize with the help of hUmp1, and propeptides of β subunits (β1, β2, β5, β6, and β7) were cleaved. hUmp1 and PAC1-PAC2 are subsequently degraded by the newly formed active 20S proteasomes.